SINGLE POINT MUTATIONS ON THE LOOP OF OXALATE DECARBOXYLASE

By

BENJAMIN THOMAS SAYLOR

A THESIS PRESENTED TO THE GRADUATE SCHOOL
OF THE UNIVERSITY OF FLORIDA IN PARTIAL FULFILLMENT
OF THE REQUIREMENTS FOR THE DEGREE OF
MASTER OF SCIENCE

UNIVERSITY OF FLORIDA

2009

To: Grandma

ACKNOWLEDGMENTS

There are many people who need to be acknowledged for their help in this work. The first is Nigel Richards. Without his advice and support, this work would not have been possible. His insight helped to keep the project on track. Also, Alex Angerhofer and Witcha Imaram have my gratitude for running and generously supplying the Electron Paramagnetic Resonance data used in this study. Finally, I thank parents for telling me to calm down and that everything will be ok.

TABLE OF CONTENTS

page

LIST OF TABLES

LIST OF FIGURES

Abstract of Thesis Presented to the Graduate School
of the University of Florida in Partial Fulfillment of the
Requirements for the Degree of Master of Science

SINGLE POINT MUTATIONS ON THE LOOP OF OXALATE DECARBOXYLASE

By

Benjamin Thomas Saylor

August 2009

Chair: Nigel Richards
Major: Chemistry

Oxalate decarboxylase (OxDC) converts oxalate to formate and CO_2. It also exhibits a small amount of oxidase activity converting oxalate to two molecules of CO_2. Previous work has identified an N-terminal active site loop that has been proposed to be important in determining the decarboxylase or oxidase activity of the protein. This loop has an extensive hydrogen bonding network and this work focused on making single point mutations to this loop with the goal of favoring the different loop conformations to favor either the decarboxylase or oxidase activities. The following four mutants: S161A, S161T, T165S, and T165V were constructed. The S161A and T165V were constructed to favor the open form of the loop and promote oxidase activity and the T165S and S161T were constructed to favor the closed form of the loop and promote decarboxylase activity.

The S161T mutant displayed kinetics similar to the His-tagged wild type enzyme for decarboxylase activity and an overall order of magnitude decrease in oxidase activity. Interestingly, S161T has the same background dye oxidation rate as the His-tagged wild type enzyme with an overall order of magnitude decrease in oxidase activity. S161A exhibits slightly increased decarboxylation activity but the oxidase activity is the same as the His-tagged wild

type enzyme. This data suggests that S161 does not play a crucial role in determining OxDC decarboxylase or oxidase activity.

T165 plays a more crucial role in determining OxDC activity. T165S when normalized for metal incorporation, behaves like the His-tagged wild type enzyme for the decarboxylation reaction. However, it displays a 300% increase in oxidase activity implying that T165 plays a small role in determining enzyme activity. T165V has only a 10^{th} of the decarboxylase activity as the wild type enzyme indicating that removal of the hydrogen bond between T165V and R92 is important for decarboxylase activity. T165V also has an order of magnitude decrease in oxidase activity compared to the His-tagged WT enzyme.

Radicals were trapped for all four mutants and the wild type protein using α-phenyl N-tertiary-butyl nitrone and subjected to electron paramagnetic resonance spectroscopy to determine if the radicals were derived from oxalate or if they derived from another source such as superoxide. Using ^{12}C oxalate, a 6 line spectrum was observed. With ^{13}C oxalate, a 10 line spectrum was observed indicating that the trapped radical came from oxalate. Overall, it was found that single point mutations favoring different loop conformations are not enough to drastically change the activity of OxDC from a decarboxylase to an oxidase.

CHAPTER 1
INTRODUCTION

Overview of Oxalate Decarboxylase, Oxalate Oxidase and the Cupin Superfamily

Oxalate decarboxylase (OxDC) catalyzes the breakdown of oxalate into formate and CO_2 as depicted schematically in Figure 1-1(*1*). Many early OxDCs were purified and characterized from various fungi such as: *Sclerotinia sclerotiorum* (*2*), *Mythrothecium verruncaria* (*3*), and *Aspergillus niger (4, 5)*. In 2000, the first prokaryotic oxalate decarboxylase was discovered in *Bacillus subtilis* (*6*). The fungi OxDC can be expressed under acidic conditions or when short chain carboxylic acids such as oxalate and glycolate are added to the growth medium (*2-5*); however, the *B. subtilis* OxDC is only expressed in acidic media and is not expressed when short carboxylic acids are added (*6*). OxDC also requires Mn(II), and dioxygen for activity, and unlike oxalate oxidases (OxOx) the oxygen is not consumed during turnover (*7, 8*).

The *B. subtilis* OxDC is a member of the cupin (Latin for small barrel) superfamily of proteins (*9*). The proteins in this family have at least one characteristic β-barrel fold. This superfamily is very diverse containing many different kinds of enzymes such as dioxygenases, decarboxylases, isomerases, and nuclear proteins (*10, 11*). The cupin β-barrel fold can also bind various metals such as Fe, Mn, Zn, and Ni which are essential to catalysis. It has been suggested that the various metals in the cupin fold contribute directly to the enzyme activity. However, not all cupins are metal binding proteins (*10, 11*).

B. subtilis OxDC is a bicupin hexameric protein containing six 44kD subunits as can be seen in Figure 1-2 (*6, 12, 13*). Each monomer contains an N-terminal and C-terminal cupin domain, both of which bind one Mn. A single OxDC monomer is presented in Figure 1-2. The N-terminal cupin metal binding site is the proposed site of catalysis based on Electron Paramagnetic Resonance (EPR) studies and kinetic simulations using GEPASI, a kinetics

modeling program (*14-16*). There is evidence based on mutagenesis studies that the C-terminal domain may possess decarboxylase activity and that the N-terminal site is not the sole site of catalysis (*17*). Also, activity at the C-terminal cupin domain cannot be fully ruled out because C-terminal mutations results in proteins that are unstable and hard to characterize (*18*). A loop in the N-terminal domain, consisting of residues 161-165, has been shown to adopt two conformations, open and closed as can be seen in Figure 1-3. It is suggested that this loop provides a solvent accessible channel to the active site. In addition, formate is bound to the active site in the N-terminal metal binding site in the open loop crystal structure (*19*). The C-terminal and N-terminal domains are structurally very similar as shown in Figure 1-4 with the Mn coordinated by three histidines and a glutamate.

OxOx is an enzyme that catalyzes the breakdown oxalate by converting oxalate to two molecules of CO_2 with reduction of O_2 to H_2O_2 as shown in Figure 1-1 (*10, 20, 21*). The *Hordeum vulgare* (barley) OxOx was predicted to be a member of the cupin superfamily based on its sequence. The crystal structure was solved and the barley OxOx was shown to be a hexameric monocupin (*22*). Early work indicated that the enzyme was activated using copper and lead (*21*); however, EPR studies showed that OxOx binds Mn(II) in the active site (*20*). Other work has focused on examining OxOx found in the fungus *Ceriporiopsis subvermispora*. Two isoforms of a bicupin OxOx where identified in *C. subvermispora*. Interestingly, these isoforms share more sequence homology with OxDC and are bicupins that exhibit a small amount of decarboxylase activity.(*23*) They also crystallized as hexamers and are able to bind Mn (*23, 24*).

The main difference between these OxOxs is in the equivalent regions to the OxDC loop. The OxOx from barley has a deletion at residues 161-162 and has no loop, but the *C. subvermispora* OxOxs have residues that could form a loop. However, this loop lacks a general

acid such as E162 and the analogous residues in *C. subvermispora* OxOxs are alanine and serine. A E162A a mutant of *B. subtilis* OxDC was constructed and it did increase the oxidase activity; thus, other residues in the loop have been predicted to be important in determining reaction specificity (*13, 23*).

The Proposed Mechanism of OxDC

OxDC converts oxalate into formate and CO_2 (*1*). In addition, *B. subtilis* OxDC also has a small amount of oxidase activity which is ~0.2% of its decarboxylase activity (*7*). The most recent mechanism proposes a branching mechanism that attempts to explain the small amount of observed oxidase activity (*15, 18*). This divergent mechanism is summarized in Figure 1-5.

The first step involves the binding of dioxygen and monopronated oxalate (fully deprotonated oxalate is not a substrate) to the Mn(II); however it is not known which binds first. The dioxygen forms a superoxide radical along with the proposed oxidation of Mn(II) to Mn(III) while the oxalate is polarized by an active site arginine at position 92 (R92). Currently, there is no direct evidence for Mn(III) formation during turnover. The terminal carboxylic acid is deprotonated by a glutamate 162 (E162) promoting a proton coupled electron transfer (PCET) leaving an oxalate radical anion. This radical anion undergoes decarboxylation aided by R92 polarization. After decarboxylation, a Mn-bound carboxyl radical anion is present. In the decarboxylation reaction it is proposed that this radical anion is protonated by E162 to form formate. In the oxidase reaction protonation does not occur, and the Mn bound carboxyl radical anion and superoxide radical react to form a five membered Mn-bound structure. This further reacts to form H_2O_2, and a second molecule of CO_2 (15, 18).

This mechanism relies on E162 and R92 for decarboxylase activity. A recent experiment that replaced the glutamate at 162 with a glutamine had significantly reduced decarboxylase activity. Most surprisingly, this E162Q mutant exhibited 0.6 U/mg of oxidase activity indicating

that this residue is important for favoring decarboxylase activity over oxidase activity (*18*). In a second set of experiments, the loop residues were sequentially mutated to similar residues found in the *C. subermispora* OxOxs. This decreased the overall decarboxylase activity and increased the oxidase activity. Surprisingly, when the E162 was reintroduced into the S161D/NS163-4SN mutant, 50% of the decarboxylase activity was restored. This further indicated that the ability of E162 to donate a proton to the carboxyl radical anion is required for decarboxylase activity (*15*).

Identification and Proposed Role of an N-Terminal Loop

In 2002 Anand and Coworkers published the first crystal structure of OxDC which is now referred to as the "open" form of the loop (*19*). They were the first to show that OxDC was a hexameric bicupin protein. At the time, the cupin domains were most similar to the monocupin forms of OxOx (such as barley) and both N-terminal and C-terminal domains shared a 15% sequence homology with OxOx (*19*). In 2005, when the sequence and crystal structures of the bicupin *C. subvermispora* OxOxs were solved it was shown that OxDC was more similar to the bicupin *C. subvermispora* OxOxs (*23*). They were also the first group to show that there was a loop at positions 161-165 of the *B. subtilis* OxDC, which provided a solvent accessible channel to the N-terminal cupin domain. However from their crystallographic results, they concluded that the C-terminal cupin domain was the active site. They based this assumption on E333 in the C-terminal domain being positioned in a way that would facilitate protonation of the carboxyl radical anion to produce formate. They ruled out the N-terminal domain as being the catalytically active domain because they do not see any residue that could act as a proton donor. In their structure, the E162 residue is rotated out of the active site in the N-terminal domain. They concluded that the C-terminal domain is the active site since E333 is positioned such that it can act as a general acid. They found that mutating E333 to alanine lowered the activity to 5% of the

His-tagged WT. They do not account for the formate seen in the N-terminal site even when no formate was added to the crystallization solution (*19*).

In 2004 Just and Coworkers, published a new crystal structure with the loop in a closed conformation and is known as the "closed" form of the loop. When the loop is closed, the solvent accessible channel is blocked from the active site. In the closed form of the loop, E162 is positioned with the oxygen of the -OH group oriented toward the active site where formate is bound in the open structure; this can be seen in Figure 1-6. They also note that the N-terminal domain has formate bound to the Mn in the open form and that the N-terminal domain, unlike the C-terminal, has an obvious solvent accessible channel. They found that N-terminal active site mutations of R92 to alanine and lysine and mutation of E162 to glutamine and alanine exhibited a V_{max} of ~1% compared to the His-tagged WT enzyme leading to the conclusion that the active site was really the N-terminal domain. From C-terminal mutations, they conclude that E333 is not the proton donor for the carboxyl radical anion because the E333A mutant still exhibits ~5% of the His-tagged WT decarboxylase activity. They propose that mutations in the C-terminal site affect the activity at the N-terminal site since E333Q has no decarboxylase or oxidase activity (*13*).

Attempts to Convert Oxalate Decarboxylase into an Oxalate Oxidase

Since OxDC possess some oxidase activity, much work has focused on trying to turn it into an oxidase through mutagenesis. The first approach involved mutagenesis of E162. The hypothesis was that mutation of E162 to E162Q would increase the oxidase activity by removing the ability of the residue to act as a general acid removing its ability to protonate the carboxyl radical anion. This approach yielded a slight increase of oxidase activity to 0.6 U/mg in one study with a reduction in decarboxylase activity to 0.5% of non-tagged WT activity (*18*).

A second approach focused on deletions and specific mutations of the N-terminal loop. The loop was shortened by deleting the residues at position 162 and 163 to make it more similar to barley OxOx which lacks a flexible loop. The decarboxylase activity dropped to 1% of the His-tagged WT activity with an increase from 0.03 U/mg to 0.08 U/mg of oxidase activity. In addition various other mutations were made for R92, E162, S161, T165. The R92 was mutated to R92A and R92K. The R92A mutant exhibited no oxidase or decarboxylase activity and the R92K mutant exhibited only 1% of His-tagged WT decarboxylase activity and no measureable oxidase activity. The metal analyses for the R92 mutants were 0.9 Mn/monomer indicating that the low activities are due to the mutations and not the lack of Mn in the active site. The S161 was mutated into S161A which exhibited 15% of His-tagged WT activity and no measureable oxidase activity. The crystal structure of S161A showed that the protein adopted the closed form of the loop and formate was seen bound to the N-terminal Mn. The last mutant on the active site loop was T165P. This mutant was constructed to favor the closed conformation of the loop while not disrupting its motions. This mutant showed 3% of His-tagged WT decarboxylase activity and the unchanged oxidase activity when compared to the His-tagged WT enzyme (*25*).

A third approach focused on mutating the loop sequentially to make it similar to the analogous residues in the *C. subvermispora* OxOx. The *C. subvermispora* OxOxs have residues that could form a flexible loop and lack a general acid at position 162. These OxOxs have serine and alanine at position 162. The residues were mutated sequentially from161 to 165. A sequence alignment of *B. subtilis, C. subvermispora, H. vulgare* loop regions is shown in Figure 1-7. The mutants exhibited an increase in oxidase activity up to 4.5 U/mg in the SENS161-164DASN with a reduction in decarboxylase activity to 0.05% of His-tagged WT activity. The next mutant, SENST161-165DASNQ, exhibited only 0.19 U/mg oxidase activity and under 0.01% of His-tagged WT dearboxylase activity. To show that E162 is important for decarboxylation, glutamate

was mutated back into the 161-164 mutant producing S161D/NS163-4SN. This mutant had 40% of the His-tagged WT decarboxylase activity and only 0.13 U/mg oxidase activity supporting the idea that E162 is important for decarboxylase activity (*15*).

Hydrogen Bonding Network in the Loop of OxDC

The open and closed crystal structures showed that the loop residues form a complex H-bonding network to other residues in the protein. Figures 1-8 and 1-9 show the proposed H-bonding interactions in the open and closed form of the loop. In the open form of the loop, S161 has the carboxyl group H-bonded to the S164 amide nitrogen and is part of a hydrogen bonding network involving a crystal water, E99, and S164's hydroxyl group. The other notable H-bond is N63's amine H-bonded to a crystal water that is bonded to the terminal carboxyl of E162; E162 has its terminal oxygen H-bonded to both the hydroxyl and amino residues on a 2^{nd} subunit T44. The T165 has no proposed H-bonds.

The closed form of the loop has a much different H-bond interactions. The S161's hydroxyl is now H-bonded to a 2^{nd} subunit T44, the terminal O^- of E67, the amide nitrogen of N163, and terminal amine of N163. Now, T165 hydroxyl has a H-bond to a crystal water that is H-bonded to the amide carboxyl groups of E162, N163, and the amide nitrogen of T165. Most importantly, this terminal hydroxyl is H-bonded to R92. This H-bond is expected to stabilize R92 and keep it in position to polarize oxalate (*12*).

Proposed Mutants and Experiments

A few different attempts have been made to convert the *B. subtilis* OxDC into an OxOx. The most promising involved mutating the *B. subtilis* OxDC loop to make it similar to the *C. subvermispora* OxOx. This increased the oxidase activity to 4.5 U/mg (*15*). However, this work did not address if only a single point mutation of the loop can switch the activity of OxDC. The only previous work on single point mutations to the loop made a few single point mutations to

the loop, S161A and T165P. In that work one of the major goals was to make a mutant, T165P, that favored the closed position of the loop. Neither of these drastically increased the oxidase activity but were shown to significantly decrease the decarbxylase activity; however, low metal incorporation cannot be ruled out since neither mutated protein was submitted for metal analysis (*25*). This work focuses on making mutants that disrupt the H-bonding to favor the open or closed from for the loop. It is proposed that S161A and T165V will should favor the open form of the loop and S161T and T165S will favor the closed form of the loop.

The work in this study is focused on making specific mutations to the active site loop that are intended to disrupt the H-bonding network of the closed form of the loop for S161A and T165V. With the close form destabilized, it is feasible for oxalate to enter the active site and consequently be decarboxylated leaving a carboxyl radical anion. Since the closed form of the loop is destabilized, E162 will be rotated away from this radical anion (see Figure 1-4) and protonation to form formate will be difficult. This should hopefully lead to the carboxyl radical getting oxidized to CO_2 with a reduction of the proposed superoxide to H_2O_2.

Two sets of mutants were created for this work. The first was a S161A and S161T pair. Even though previous studies have been done on S161A it is worth repeating the work. The previous work on S161A was part of a larger experiment to show that the N-terminal site was the primary active site and did not focus on trying to increase the oxidase activity. In addition, the S161A was not fully characterized because it lacked a metal analysis. The hypothesis is the lack of hydroxyl H-bonds in the closed form of the loop for S161A would lead to a destabilization of the closed loop which would lead to a decrease in decarboxylase activity and an increase in oxidase activity. The S161T should behave similar to wild type because threonine should be able to H-bond with the network similar to the WT but it might not bond as well due to the methyl group. This methyl group could have steric interactions which would rotate the hydroxyl group

slightly so the H-bonding would not be as strong. This mutant was expected to have slightly lower decarboxylase activity and slightly higher oxidase activity.

The next set of mutants involves mutating T165V and T165S. The previous mutant T165P was designed to favor the closed form of the loop. The T165V mutant is designed to disfavor the closed form of the loop and favor the open form of the loop. The hypothesis is that the T165V mutant will have very low decarboxylase activity and hopefully higher oxidase activity since E162 is rotated away from the radical anion. Also, removing the hydroxyl group is proposed to favor the open form of the loop; once again, rotating the E162 away from the carboxyl radical anion. In this case the T165S is expected to H-bond to R92 and should behave similar to the WT enzyme. However, this might make the loop adopt a slightly different conformation since the methyl group is replaced by a hydrogen removing possible steric clashes.

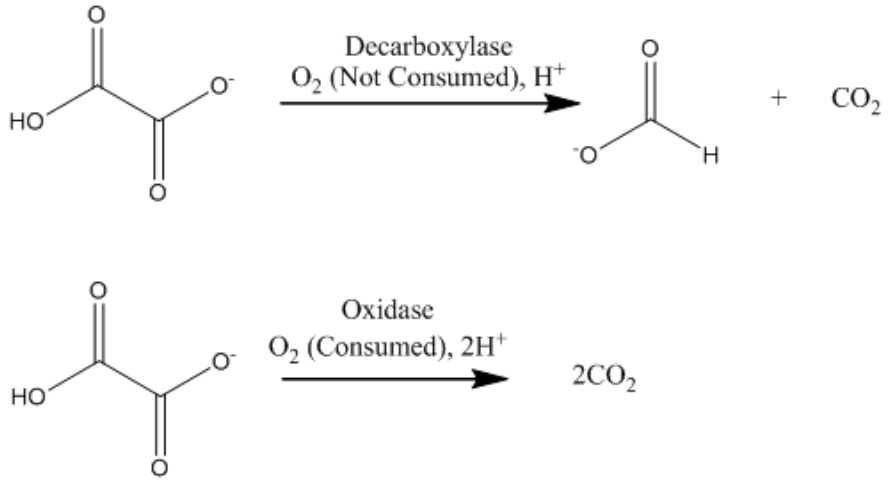

Figure 1-1. The overall reaction catalyzed by OxDC and OxOx.

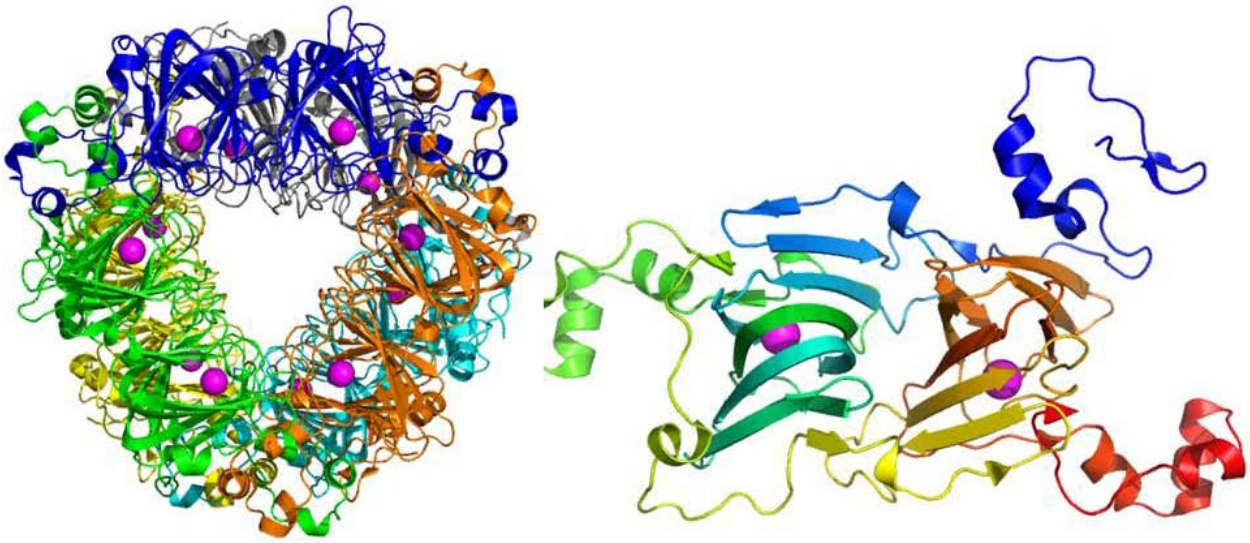

Figure 1-2. The hexamer is on the left. The hexamer was constructed from the open form of the enzyme (PDB Code 1J58). Each color represents one OxDC subunit. The Mn is shown in purple. The momomer is one subunit from the overall hexamer with the N-terminal colored blue and following the colors of the rainbow to the C-terminal which is colored red. Figure made in Pymol (*26*)

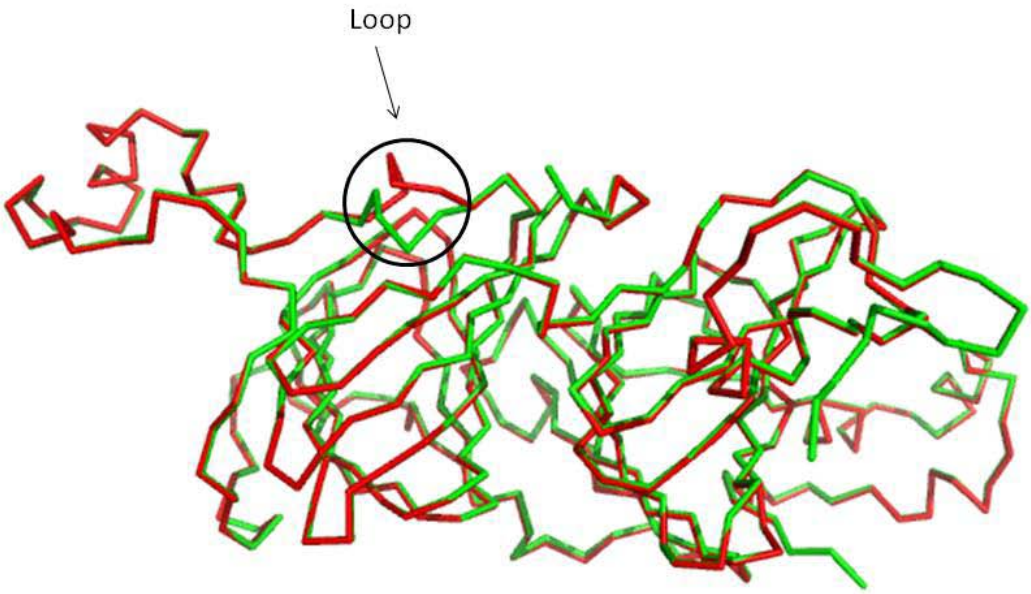

Figure 1-3. Crystal structure alignment of the open and closed loop conformations of OxDC. The open form is shown in shown in red and the closed form is shown in green. The structural alignment was done using Pymol (PDB Codes 1J58 and 1UW8) (*26*)

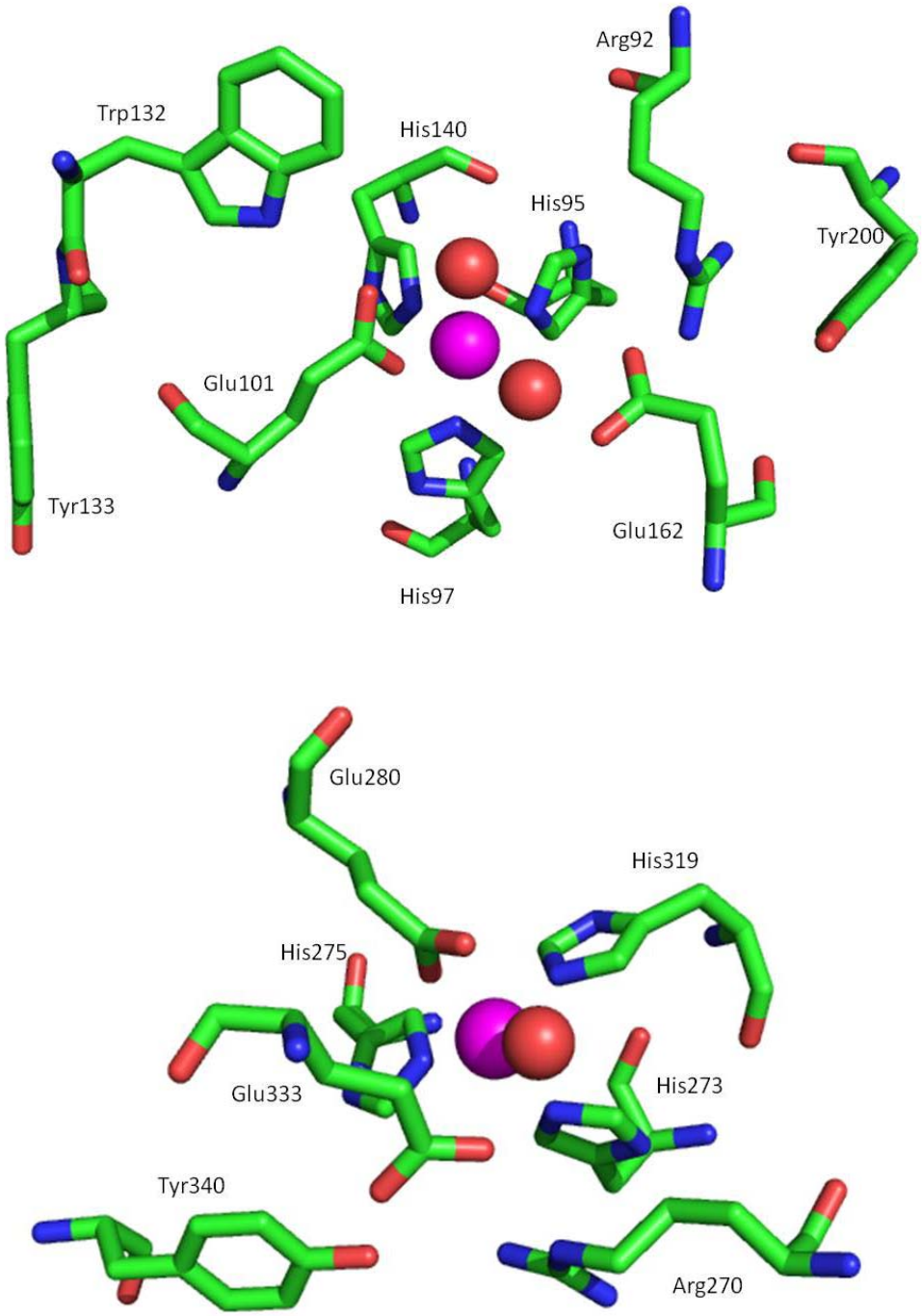

Figure 1-4. N-terminal and C-terminal metal binding sites (PDB Code 1J59). The N-terminal is on top and the C-terminal is on bottom. The Mn is shown in magenta and the oxygen of the crystal waters is shown as a red sphere. Figure generated in Pymol (*26*)

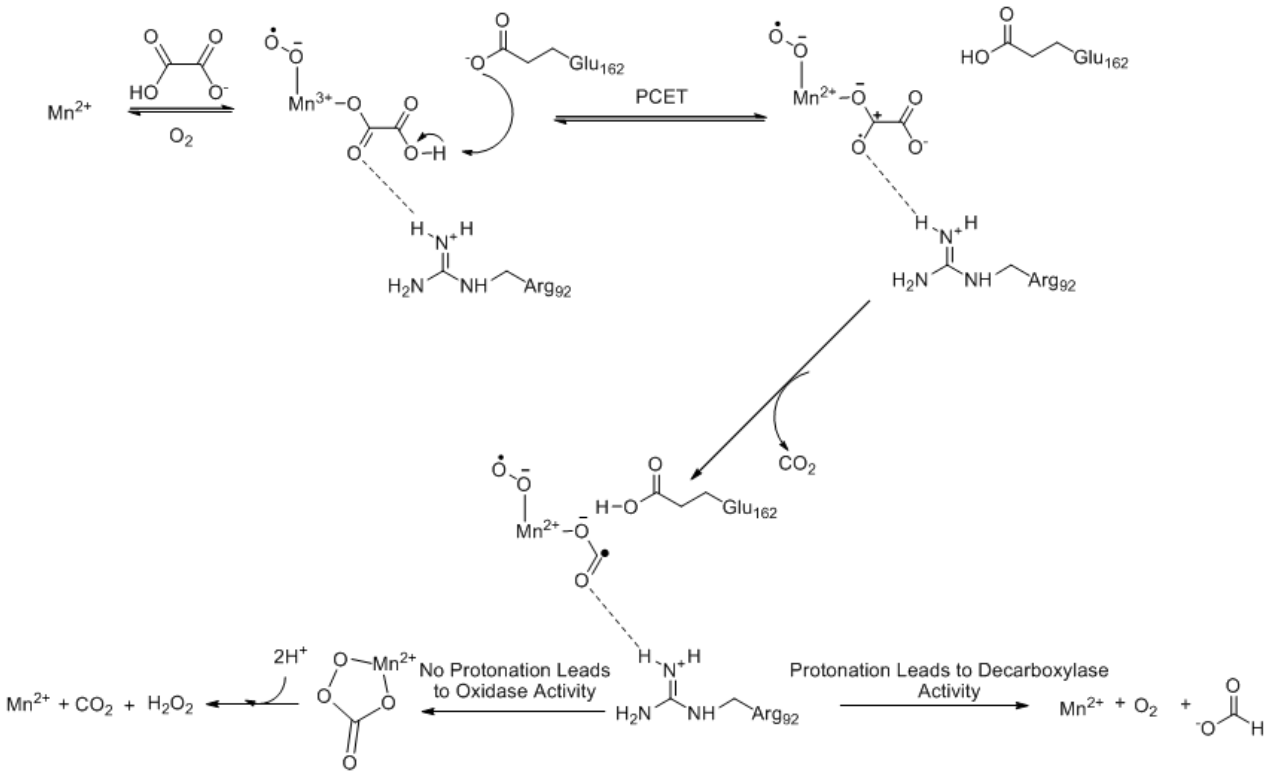

Figure 1-5. Proposed divergent mechanism of OxDC (Adapted from References (*15*, *18*)

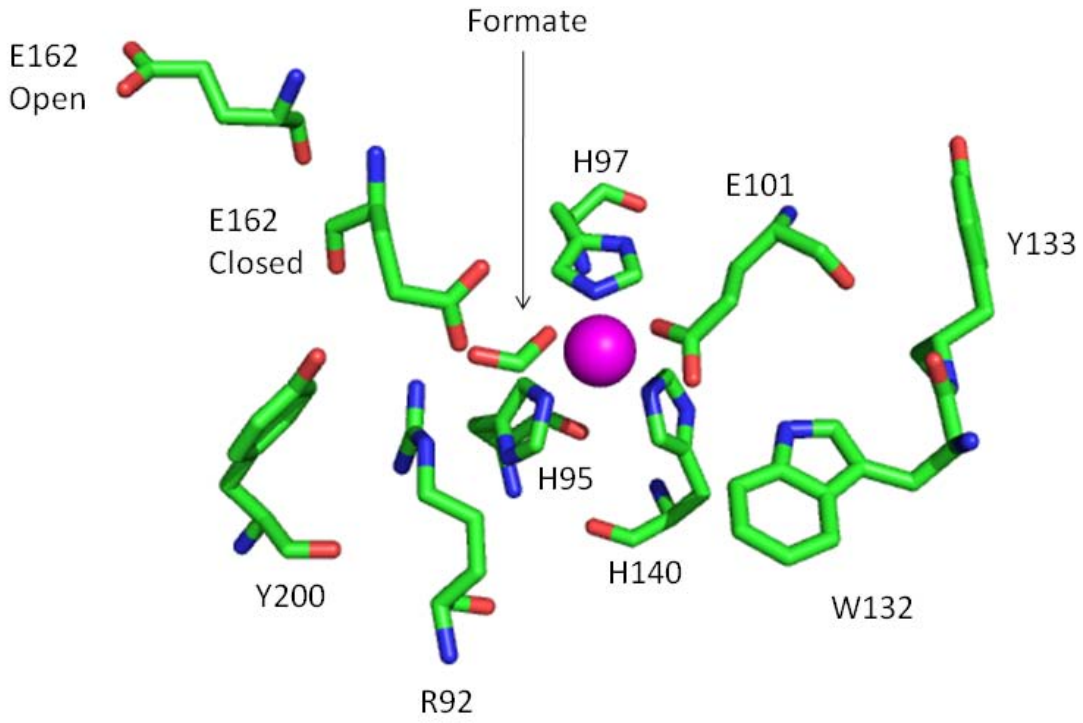

Figure 1-6.The N-terminal active site of OxDC showing the position of E162 in both the open and closed conformations. Formate was placed in the active site based on its location in the closed loop OxDC crystal structure and the active site residues are shown for the closed loop conformation (PDB Codes 1J58 and 1UW8)

```
B.subtilisOxDC              FDDGSFSENSTFQLTD
C.subvermisporaOxOx-G       FPDGTFDASNQFMITD
C.subvermisporaOxOx-C       FPDGTFDSSNQFMITD
H.vulgare                   FNSQNP---GIVFVPL
```

Figure 1-7. Sequence alignment of *B. subitlis* OxDC, *C. subvermis*ora OxOx's, and *H. vulgare* using ClustalW2 (*27*).from Burrell Biochemistry, 2007 (*15*)

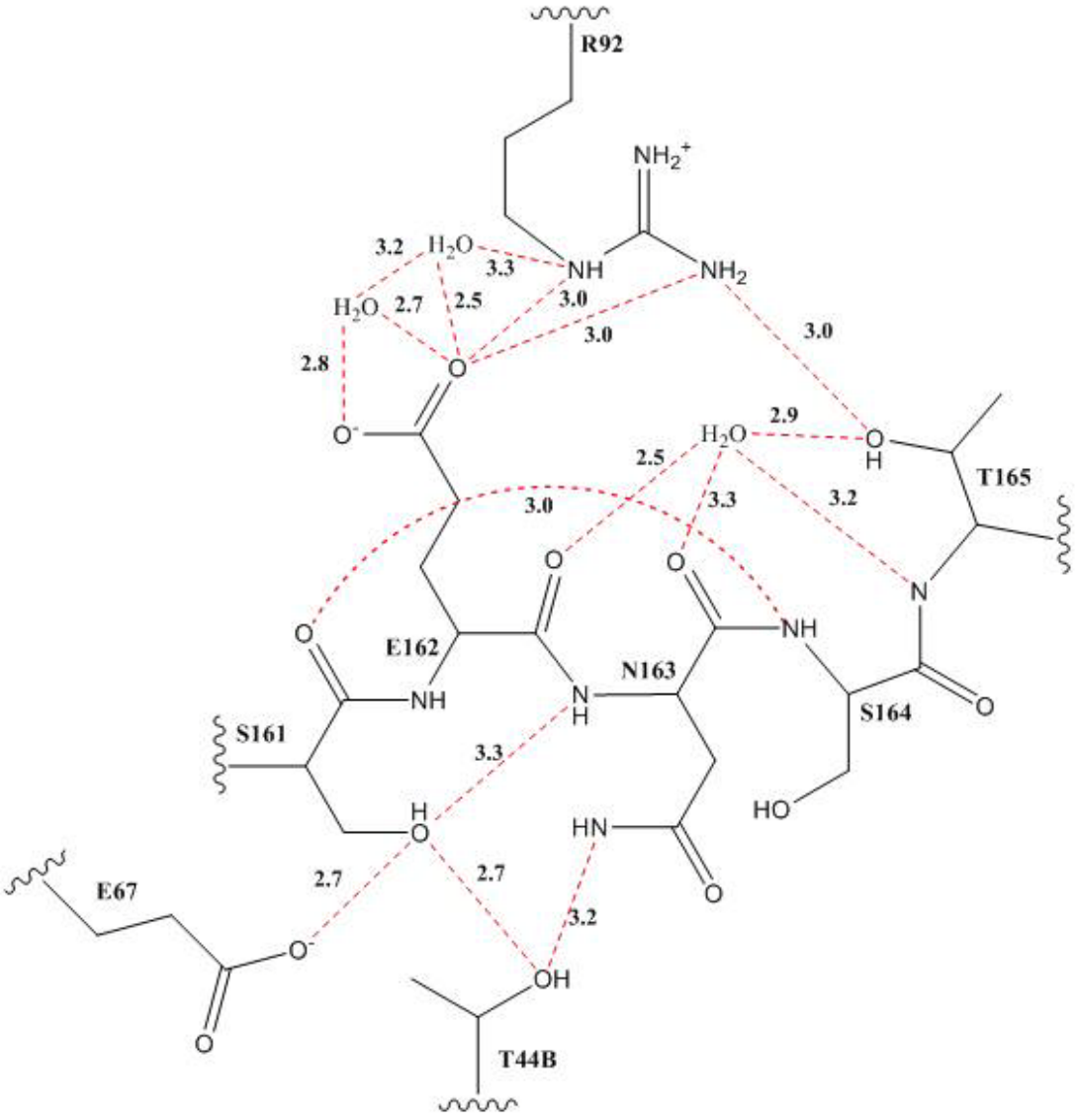

Figure 1-8. Hydrogen bonding network of the closed form of the loop (Adapted from Burrell (*12*)

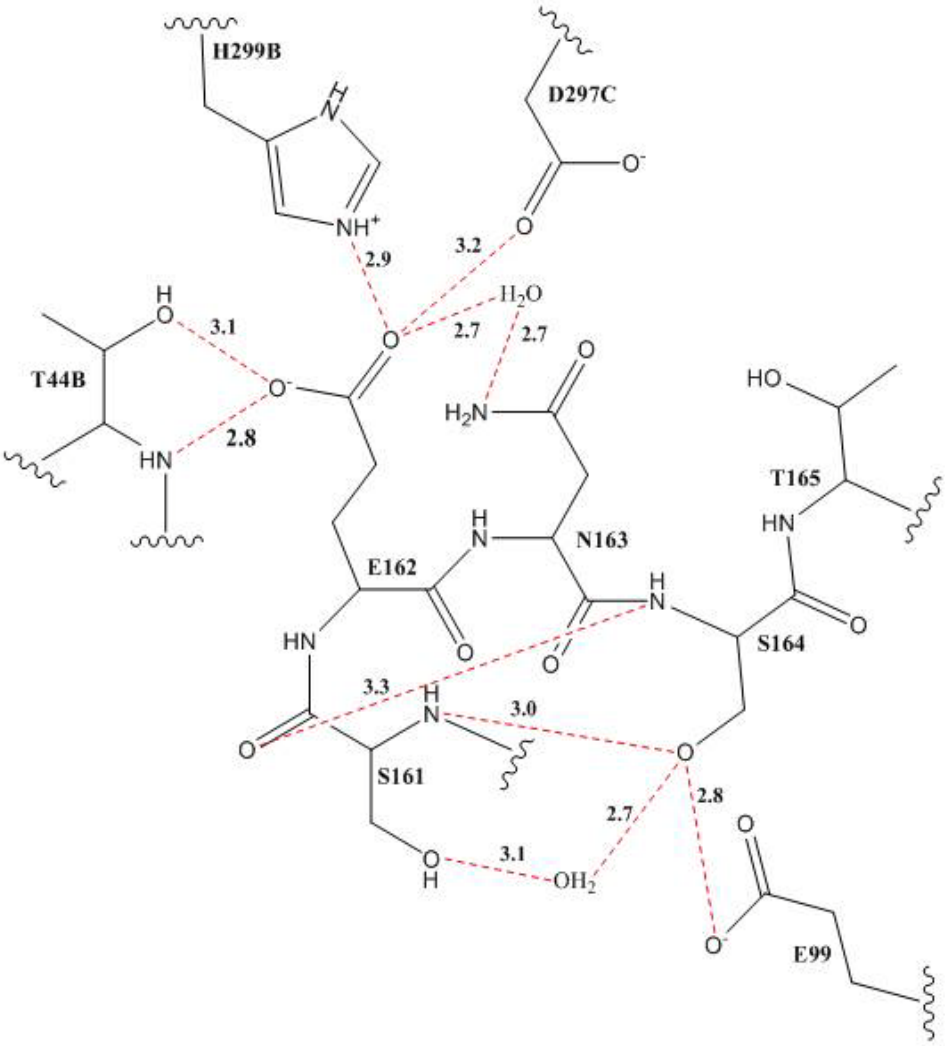

Figure 1-9. Hydrogen bonding network of the open form of the loop (Adapted from (*12*)
Residues ending in B and C are from the second and third subunits of the hexamer.

CHAPTER 2
MATERIALS AND METHODS

General Experimental

All materials were purchased from Fisher Scientific unless otherwise noted and were of the highest quality available. The nickel-nitrilotriacetic acid agarose (Ni-NTA) was from Qiagen. Milli-Q water, 18 Ω, was used exclusively for purification and kinetic work. All spectra were recorded on an Agilent 8453 UV/Vis spectrometer. Primers were designed using Generunner version 3.05 (Hastings Software, Inc) and purchased from Integrated DNA Technologies.

QuickChange Mutagenesis

The QuickChange was done following the Stratagene procedures.(*28*) The following primers were used for QuickChange with mutated base underlined:

Primers S161A:

Forward: 5′-GGATCATTCGCTGAAAACAGCACGTTCC-3′

Reverse: 5′-GGAACGTGCTGTTTTCAGAGCATGATCC-3′

Primers S161T:

Forward: 5′-GGATCATTCACTGAAAACAGCACGTTCCA-3′

Reverse: 5′-TGGAACGTGCTGTTTTCAGTGAATGATCC-3′

Primers S164A:

Forward: 5′-TCTGAAAACGCCACGTTCCAGCTGACAG-3′

Reverse: 5′-CTGTCAGCTGGAACGTGGCGTTTTCAGA-

Primers T165S:

Forward: 5′-CTCTGAAAACAGCAGCTTCCAGCTG-3′

Reverse: 5′-CAGCTGGAAGCTGCTGTTTTCAGAG-3′

Primers T165V:

Forward: 5′-CTGAAAACAGCGTGTTCCAGCTGAC-3′

Reverse: 5′-GTCAGCTGGAACACGCTGTTTTCAG-3′

The Polymerase Chain Reactions (PCR) were conducted in a 50 µL volume containing 125 ng of forward and reverse primers, 10 ng of template DNA, pET9a with non-tagged WT OxDC, 5 µL 10x *PfuTurbo* AD buffer, 30 µL of water, 0.25 mM dNTP mixture, and 1 µL of *PfuTurbo* AD (Stratagene) polymerase. The mixture was heated to 95^{o}C for 2 min before being cycled 16 times at 95^{o}C for 30 sec, 55^{o}C for 1 min, 72^{o}C for 6 min. The template DNA was digested using *DpnI*. JM109 (Novagen Madison, WI) chemically competent cells were transformed with mutated DNA by incubating with 3 µL of digested PCR mixture on ice for 30 min before heat shocking at 42^{o}C for 30 seconds. Super Optimal Broth with Catabolite Repression Media (SOC) was added and the cells were allowed to recover at 37^{o}C for 1 hour with shaking before being platted onto Luria broth with ampicillin media (LBA) and incubated overnight at 37^{o}C. Isolated colonies were grown overnight in 50 mL of LBA and DNA was isolated using a Promega Wizard Kit (Madison, WI).

Overlap Extension Mutagenesis and Plasmid Purification

The following method is a variation on the overlap extension method and was used to construct the mutants used in this study (*29*). The mutants were made from the following primers and the underline regions indicate the bases that were changed and bold regions indicate the restriction sites:

OxDC Forward NdeI:

5′-GGAGGAAAC**ATCATATG**AAAAAACAA-3′

OxDC Reverse XhoI:

5′-GTGGTG**CTCGAG**TTTACTGCATTTC-3′

T165V:

Forward: 5′- AGCGTGTTCCAGCTGACAGATTGG -3′

Reverse: 5′-GAACACGCTGTTTTCAGAGAATGATCC-3′

S161A:

Forward: 5′-ATTCGCTGAAAACAGCACGTTCCA G-3′

Reverse: 5′-TGTTTTCAGCGAATGATCCATCGT C-3′

S161T:

Forward: 5′-ATTCACTGAAAACAGCACGTTCCAG-3′

Reverse: 5′-TGTTTTCAGTGAATGATCCATCGTC-3′

T165S:

Forward: 5′-AGCAGTTTCCAGCTGACAGATTGG-3′

Reverse: 5′-GAAACTGCTGTTTTCAGAGAATGATCC-3′

PCRs were conducted in a 50 µL volume containing 40 µL H_2O, 5 µL of *PfuTurbo* AD 10x buffer, 50 ng of template OxDC in pET9a, 0.25 mM dNTP mixture, 0.2 µM of forward primer, 0.2 µM of reverse primer, 1 µL of *PfuTurbo* AD enzyme. The template DNA was generously provided by Mario Moral and Patricia Moussatche. The first set of PCR reactions were run for two minutes at 95 ^{o}C and then 30 cycles of denaturing at 95^{o} C for 30 seconds, annealing at 60 ^{o}C for 30 seconds, and extension at 72^{o}C for 1 min, and then a final extension at 72^{o}C for 10 min before cooling to 4^{o}C. The S161T mutant required an annealing temperature of 55^{o}C. A second set of PCR reactions was conducted to stitch together the two PCR products

from the first round. The second PCR was conducted in a 50 µL volume containing 40 µL H_2O, 5 µL *PfuTurbo* AD 10x buffer, 1 µL of each of the first round PCR mixtures, 0.2 mM dNTP mixture, 0.2 uM of OxDC forward *NdeI* primer, 0.2 µM OxDC *Xho*I reverse primer, and 1 µL *PfuTurbo* AD. The second PCR reaction was run for 2 min at 95 ^oC and then 30 cycles of denaturing at 95^o C for 30 seconds, annealing at 60 ^oC for 30 seconds, and extension at 72^{o}C for 1 min Followed by a final extension at 72^{o}C for 10 min before being cooled to 4^{o}C indefinitely. The final PCR was cleaned up using a Wizard Kit from Promega. The purified DNA was cut at 37^{o}C for 1-2 hours using *Xho*I and *Nde*I (New England Biolabs). The DNA was ligated into pET32a (Novagen) previously cut with *Nde*I and *Xho*I and treated with calf intestinal alkaline phosphatase treated using T4 DNA ligase (New England Biolabs), at room temperature for 15 min. JM109 was transformed with 1-5 µL of the ligation mixture and plated on LBA and grown at 37^{o}C overnight. Colonies were grown in Terrific Broth (TB) and screened following the procedure in Maniatis (*30*). Colonies containing insert were grown in 50 mL LBA overnight at 37^{o}C and the plasmid purified using a Wizard Midiprep Kit (Promega). Plasmid DNA was sequenced by the University of Florida Sequencing Core.

Purification of His-Tagged OxDC and His-Tagged OxDC Mutants

Purified pET32a DNA was transformed into competent BL21(DE3) (Novagen) cells and grown on LBA overnight at 37^{o}C. A single colony was selected and grown overnight in 50 mL of LBA at 37^{o}C. Three flasks containing 475 mL of LB were inoculated with 6 mL of overnight culture and allowed to grow to an OD_{600} of ~0.4. The bacteria were heat shocked at 42^{o}C for 18 min with manual swirling every two min. before addition of 5 mL of 0.1 M Isopropyl β-D-1-thiogalactopyranoside (IPTG) and 2.5 mL of 1 M $MnCl_2$. The final concentrations were 1 mM IPTG and 5 mM $MnCl_2$. The cells were incubated for an additional 4 hours at 37^{o}C with shaking. The cells were harvested on a Sorvall RC-B Plus at 6000 x g for 18 min at 4^{o}C and stored at

-20°C. The cells were thawed and resuspended in 60 mL lysis buffer containing 50 mM Tris-Cl pH 7.5, 0.5 M NaCl, 10 µM $MnCl_2$, and 10 mM imidazole. The cells were sonicated using 4 x 20 sec cycles at 70% amplitude on a Sonic Demembrator 500 (Fisher Scientific). Cellular debris was removed by centrifuging at 13,000 g for 18 min a 4°C. The lysate was loaded onto a Ni-NTA (Qiagen) column previously equilibrated in lysis buffer. The column was washed with 50 mM KPi pH 8.5, 0.5 M NaCl, and 20 mM Imidazole. The protein was eluted using 50 mM KPi pH 8.5, 0.5M NaCl, 250 mM Imidazole. Fractions containing the OxDC were pooled and Chelex 100 Resin (Bio-Rad) was added to remove advantageously bound metals. Metal free storage buffer, 50 mM Tris-Cl pH 8.5, 0.5 M NaCl, was prepared by eluting the buffer through Chelex 100 Resin following the manufacturer's instructions. The protein was buffer exchanged into the metal free 50 mM Tris-Cl pH 8.5, 0.5 M NaCl using a G-25 column with the resin having been soaked in 1 M ethylenediaminetetraacetic acid (EDTA). The EDTA was used to remove any metal ions bound to the G-25 resin. The fractions containing OxDC were pooled, and if needed concentrated using an Amicon Centriprep YM-30 (Millipore). The His-tagged WT enzyme was stored at ~4 mg/mL and the mutants stored at 5.5-10 mg/mL for kinetic work. Samples for EPR were between 6-15 mg/mL. All proteins were stored at -80°C until used. Protein samples were submitted for inductively coupled plasma mass spectrometry metal analysis at the University of Wisconsin Soil and Plant Analysis Lab (Verona, WI).

Protein Concentration Using the Bradford Assay

The concentration of the protein was determined by examining the absorbance at 595 nm due to the binding of Coomassie Plus Protein Assay Reagent (Thermo Scientific) to the protein (*31*). A standard curve was made using bovine serum albumin. The standard curve was made fresh at the same time the unknown samples were prepared.

OxDC Decarboxylase Activity Assay

Assays were run in 100 µL volume containing 50 mM sodium acetate, 0.5 mM *o*-phenylenediamine, 0.2% Triton-X 100, 2.5-100 mM potassium oxalate pH 4.2, H_2O, and 4-9 ug of enzyme to initiate the reaction. After a certain interval of time, the reaction was quenched by addition of 10 µL of 1.1 M sodium hydroxide. The formate in these samples was assayed using an end point assay with formate dehydrogenase. A 55 µL aliquot of the OxDC assay was brought to 1 mL with final concentrations of the following: 47.5 mM KPi pH 7.8, ~0.2 units formate dehydrogenase (FDH), 0.09 mM NAD^+, and H_2O. This solution was incubated overnight at 37^{o}C. A standard curve was constructed each time by spiking with a known amount of formate and performing the FDH assay. The amount of formate in each sample was determined from examining the production of NADH at 340 nm. All graphs to determine K_m and V_{max} were done in Kaleidagraph version 3.5 (Synergy Software) using the Michaelis-Menten fitting model. All data points were done in triplicate.

OxDC Oxidase Activity Dye Oxidation Assay

Assays were run in 1 mL volume containing 50 mM sodium acetate pH 4.0, 20 mM potassium oxalate pH 4.0, 5 mM 2,2'-azino-bis(3-ethylbenzthiazoline-6-sulphonic acid) dye (ABTS), 25 units horseradish peroxidase type VI-A (Sigma-Aldrich) (HRP), and 6-18 ug of enzyme. The reactions were run at 23^{o}C. The reaction was initiated by addition of the enzyme, and the absorbance of the oxidized ABTS was monitored at 650 nm for 45 seconds. The molar absorptivity of ABTS was considered to be 10,000 M^{-1} cm^{-1} (*20*). Since OxDC can oxidize dyes during turnover, two controls were run.(*14*, *15*) One control involved running the reaction without the HRP to get the background rate of dye oxidation during turnover and a second control reaction was run omitting oxalate. The control without the HRP reaction rate was subtracted from the reaction rate of the full HRP dye oxidation. The second control had a rate of

near zero and was not subtracted from the measured activity. All reactions were done in duplicate.

OxDC Oxidase Activity Using a Clark Type Oxygen Electrode

Oxygen consumption of the T165V and T165S mutants was measured using a Clark Type Oxygen Electrode (*32*). An Instech Labs Batch Flow System with 125/05 Y oxygen electrode connected to a Yellow Springs Instruments 5300 A Biological Oxygen Monitor was used to measure the oxygen consumption. The temperature of the system and solutions were equilibrated to 23^{o}C using a water bath. The electrodes were bridged by a KCl solution (prepared fresh) and contained using a membrane. In addition, the voltage was maintained at 0.7 V using the YSI 5300A. The system was zeroed in a solution of buffer with sodium dithionite to set the 0% reading and then an air saturated buffer solution was used to set the 100% reading. Into the system, 150 µL of 200 mM sodium acetate pH 4.2, 390 µL of water, and 12-20 ug of enzyme were added. The system was allowed to equilibrate for 10-15 min. until the readout stabilized. Then 60 µL of 200 mM potassium oxalate pH 4.2 was added and the oxygen consumption monitored. The initial oxygen concentration was assumed to be 250 µM (*33*) or 0.15 µmoles in 600 µL.

EPR Spectrum

EPR spectra were obtained by Alex Angerhofer and Witcha Imaram at the University of Florida. They generously provided the figures as well.

CHAPTER 3
RESULTS AND DISCUSSION

QuickChange Mutagenesis

Mutagenesis was carried out as described in Chapter 2. The Quickchange method relies on mutating the DNA at a specific location with the polymerase copying the entire plasmid. After PCR, this leaves a nicked plasmid product and the initial methylated template. *DpnI* digests the methylated template leaving only the nicked PCR product. The product is ligated and an *E. coli* strain that can fix the nick, such as JM109, is transformed with the ligated DNA. A summary of this method is shown in Figure 3-1.

Only T165V, T165S, and S161T produced colonies. Even after multiple attempts, S161A never yielded a QuickChange colony. Figure 3-2 shows the isolated DNA. No band appears for the PCR product which should show up around 6000 bases. Most of the isolated DNA is sheared genomic DNA since RNAase did not remove the streaks. The cells were only grown in LB broth for this experiment.

Overlap Extension Mutagenesis

Overlap extension involves running two initial PCR reactions where the internal primers overlap by ~10 bases. The first PCR reaction amplifies pieces of DNA shorter than the overall gene. For this PCR, one reaction uses an internal reverse primer and an external forward primer and the other uses an internal forward primer and an external reverse primer. The internal primers contain the mutation in their sequences. This creates two pieces of overlapping DNA. In a second PCR reaction, these overlapping pieces are used as the template. The PCR product from the second step is the full length of the gene and incorporates the mutation. The PCR product is then cut with appropriate restriction enzymes and ligated into an appropriate vector. Figure 3-3 is

a summary of this method. One major advantage of this method is the PCR products in all steps can be readily visualized on a DNA gel.

In the first reaction the annealing temperature needed to be varied between 55-60^{o}C. The S161T mutant required an annealing temperature of 55^{o}C or else no product was obtained. The other four mutants required 60^{o}C annealing temperatures. Ligation into pET32a was inefficient. Only about 20% of screened colonies showed an insert. The pET32a vector is a medium copy vector with only 20-40 copies per cell (*34*). Use of regular LB media yielded no hits for any of the colonies. It was possible that hits were present but the DNA concentration was too low to be visualized on a gel. All screening and purification of the plasmids had to be conducted in Terrific Broth (TB). The TB allows for higher cell density and more copies of the plasmid. The use of TB resulted in concentrations of plasmid DNA that could be visualized during screening and a high enough concentration for sequencing. Use of TB yielded DNA concentrations of 400-800 ng/µL recovered from midiprep purifications while LB midiprep yielded only ~50-100 ng/µL.

The PCR products were also the correct size. Using a reverse internal primer and an external forward primer, a product of ~480 bases was obtained and when using a forward internal primer and an external reverse primer a product of ~540 bases was obtained. After the second round of PCR a product ~1100 bases was obtained which is the approximate size of the OxDC gene. A representative gel for the overlap extension method used in this work is shown in Figure 3-4. All genes where sequenced to verify that the desired mutation was present and no other mutations were present.

Purification of OxDC and the Mutants

The His-tagged WT and mutants were purified from 1.5 L of LB culture of BL21(DE3) *E. coli* using a Ni-NTA column to trap the 6x histidine tag on the C-terminal end of the protein. Figure 3-5 shows a representative gel of OxDC purification. Some protein was always seen in

the flow through and the wash but did not significantly decrease the amount of purified protein. The final yields of the His-tagged WT and mutants were similar with about 20 mg per liter of culture. A pool of enzyme was taken for kinetics when the concentration reached 4-6 mg/mL. The protein was further concentrated for EPR to 8-15 mg/mL. The S161A was not concentrated past 6 mg/mL due to precipitate formation. No other mutant precipitated during purification and concentration. Table 3-1 lists the final concentrations of the enzyme for both kinetic and EPR experiments along with the total amount of protein recovered. The His-tagged WT OxDC and the mutants migrated the same distance on a SDS-PAGE gel as can be seen in Figure 3-6. The estimated size of the wild type and mutants is 44 kD.

Oxidase Activity by the Oxygen Electrode

A Clark Type Oxygen Electrode (*32*) has a platinum cathode and a Ag/AgCl anode and uses a Ag/AgCl reference electrode. The electrodes are covered by a thin Teflon membrane using a half saturated potassium chloride solution to bridge the electrodes. A controller is used to apply a voltage across the electrodes. The oxygen diffuses across the membrane and undergoes the reaction in Figure 3-7. The current that is produced is proportional to the concentration of dissolved oxygen and is measured using a detector. The solution is constantly stirred in order for the oxygen diffusion to remain at a steady rate (*35*). The oxygen measurement is temperature sensitive with a drift of 4% per 1^{o}C (*36*). Therefore, a water bath was used to keep the temperature of the system constant at 23^{o}C and all solutions were equilibrated to 23^{o}C before use. Only T165S and T165V's oxidase activities were studied using the oxygen electrode. For these experiments the concentration of dissolved oxygen was assumed to be 250 µM (*33*) or 0.15 µmoles in 600 µL.

Table 3-2 lists the specific activities for oxidation of these two mutants. Figure 3-8 and 3-9 show the oxygen consumption for T165S and T165V respectively. The T165V graph shows no

measureable oxygen consumption and is flat; the slight measured decrease in oxygen is due to electrode drift. Even when holding the temperature constant the electrode would tend to drift ~0.3% per min. However, the T165S graph shows an increase in oxidase activity and a measureable consumption of oxygen. The measured oxdiase activity of the T165S was 0.38 U/mg; the oxygen consumption of T165S starts to curve away from linearity after about 50 seconds. Therefore, the specific activity was calculated at 45 seconds. These measurements provide evidence that the T165S has an increased oxidase activity.

Oxidase Activity Measured by ABTS Dye Oxidation

The oxidase reaction produces H_2O_2 and this production can be monitored by using an ABTS dye oxidation system involving horseradish peroxidase. Horseradish peroxidise reacts with the H_2O_2 to form two molecules of H_2O during this reaction it oxidizes the ABTS dye. This change can be measured at 600 nm and the rate of H_2O_2 production from OxDC turnover calculated. A summary of this reaction appears in Figure 3-10. OxDC can oxidize ABTS during turnover so a control experiment was conducted to assay and subtract the background rate of ABTS oxidation during OxDC turnover. For some mutants, this background oxidation can be over 0.3 U/mg. A second control was conducted to examine oxidation of ABTS dye with no OxDC present to make sure the dye is not oxidizing in the buffer with HRP present. The second control reaction was always significantly slower than the first control. Thus, the first control rate was subtracted from the measured ABTS oxidation rate to calculate the oxidase activity. The oxidase activities and the backgrounds are shown in Table 3-3.

The oxidase activity of the His-tagged WT enzyme was measured to be 0.28 U/mg which is higher than reported in the literature but similar to the 0.14 U/mg previously measured in our lab (Moomaw unpublished result). The S161A mutant exhibited oxidase activity that was the same as the His-tagged WT enzyme of 0.24 U/mg while the S161T and T165V both had

extremely low oxidase activities of 0.014 and 0.002 U/mg respectively. The interesting mutant is T165S. This mutant exhibited an increase in oxidase activity to 0.75 U/mg, three times the activity of the His-tagged WT enzyme. It is the only enzyme to have increased oxidase activity in this study. The increased oxidase activity for this mutant was seen in the oxygen electrode experiments as well.

Decarboxylase Activities of OxDC and the Mutants Using a FDH Coupled Assay

The decarboxylase activity was measured using a stopped assay and measuring formate production with formate dehydrogenase (FDH). In the first step of this assay, OxDC converts oxalate to formate and CO_2 and the reaction is quenched with NaOH. The formate is then quantified using FDH which converts the formate to CO_2 with a reduction of NAD^+ to NADH. The reduced NADH can be measured at 340 nm and the decarboxylase activity calculated. The coupled reactions are shown schematically in Figure 3-11. The decarboxylase activities and kinetic parameters are shown for all the enzymes in Table 3-4 and the Michaelis-Menten curves are shown Figures 3-12 through 3-16.

The His-tagged WT enzyme in this study behaved similarly to the non-tagged WT. For a metal incorporation of 1.4 Mn/monomer an activity of 30-35 U/mg would be expected (*14*) similar to what was measured. In addition the K_m was found to be 18 mM which is close to the reported literature values ranging from 6-16 mM for the His-tagged enzyme (*12*, *14*, *37*).

All of the enzymes but T165V exhibit significant decarboxylase activity. The T165S has the lowest specific activity of the active mutants with 23 U/mg. However, when this is normalized for Mn incorporation the activity is slightly higher than His-tagged WT enzyme indicating that the lower activity is due to low metal incorporation and is not due to the mutation of the enzyme. In addition, the k_{cat}/K_m for T165S is 2100 M^{-1} sec^{-1} which is similar to 1600 M^{-1} sec^{-1} for the His-tagged WT enzyme.

T165V has low decarboxylase with a specific activity of only 4.6 U/mg which is 11-12 times lower than the His-tagged WT with similar metal incorporation. Interestingly, this mutant does not possess low metal incorporation; it has the highest metal incorporation of any of the enzymes used in this study. Therefore, the lower activity is not due to a lack of Mn but due the mutation. The k_{cat}/K_m for this mutant is 140 M^{-1} sec^{-1}, which is only a tenth of the His-tagged WT value.

The S161A and S161T mutants both behave similarly to the His-tagged WT enzyme. The S161T mutant has a k_{cat}/K_m of 1900 M^{-1} sec^{-1} which is very close to the His-tagged WT value. Also, the K_m for this mutant is 21 mM compared to the His-tagged WT 18 mM and it bound 1.5 Mn/monomer. The S161T mutant is kinetically indistinguishable from the His-tagged WT enzyme. The S161A is slightly faster when compared to the His-tagged WT enzyme. Previous work reported that this enzyme was only 15% as active as the His-tagged WT but no metal analysis was reported for this enzyme (*25*). The S161A exhibited a k_{cat}/K_m value of 6000 M^{-1} sec^{-1}. Also, the K_m for this enzyme was lowered to 6 mM. A K_m of 6 mM has been reported for other batches of the His-tagged WT enzyme.

Spin Trap EPR Using N-tertiary-butyl Nitrone

In the proposed mechanism of OxDC, a superoxide and a carboxyl radical are proposed to be generated. One of the goals of this work was to examine the ability of α-phenyl N-tertiary-butyl nitrone (PBN) to trap radicals during enzyme turnover. Figure 3-11 depicts the PBN radical reacting with a carboxyl radical to from the spin trap product examined by EPR.

Two series of spin trapping were conducted. In the first series, PBN was mixed with the enzyme and ^{12}C oxalate. The reaction time was varied in both sets so that similar amounts of oxalate would be consumed, and the pH was monitored to ensure it stayed around 4.2. The EPR for this series is depicted in Figure 3-18. The second set of spin trapping involved using ^{13}C

oxalate with the enzyme. If the trapped radical comes from oxalate, this radical would change the splitting pattern in the spectra. The ^{13}C oxalate EPR spectra are presented in Figure 3-19.

The PBN spin trap was able to trap a radical for all the enzymes. The His-tagged WT OxDC has the least amount of radical trapped while the T165V had the most radical trapped. The S161A also had more radical trapped than S161T and T165S. The radical trapped for the ^{12}C oxalate experiments appears to be the same for the His-tagged WT and mutants. The PBN trap product gives a 6 line EPR spectrum for all the radicals with the peaks at the same magnetic field. Using ^{13}C oxalate, the His-tagged WT had the least radical trapped and T165V had the most. The trapped radical was the same for the His-tagged WT and mutants and gave a 10 line spectrum.

The trapped radical appears to originate from oxalate. If the trapped radical is not from oxalate then using ^{13}C oxalate should not affect the spectrum. However, when ^{13}C oxalate is the reagent, the trapped radical signal is different. Instead of a 6 line EPR spectrum a 10 line spectrum is observed. This extra splitting is due to the nuclear spin of ^{13}C. Thus, the radical that is trapped must be derived from oxalate.

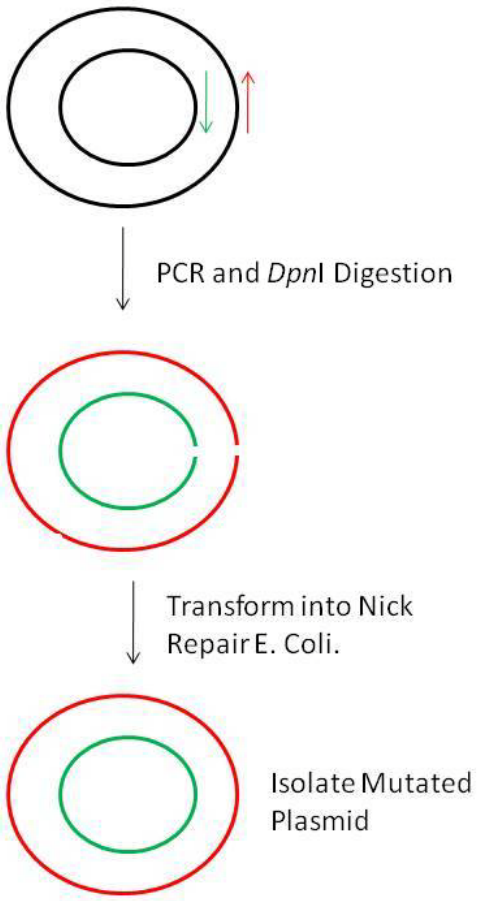

Figure 3-1. Summary of QuickChange method. Two primers are used (Red and Green) and PCR is conducted to produce a nicked mutated plasmid. This plasmid is then transformed into bacteria that can repair the nicked plasmid. The plasmid is then isolated from the bacteria. This figure was adapted from the Stratagene manual (*28*)

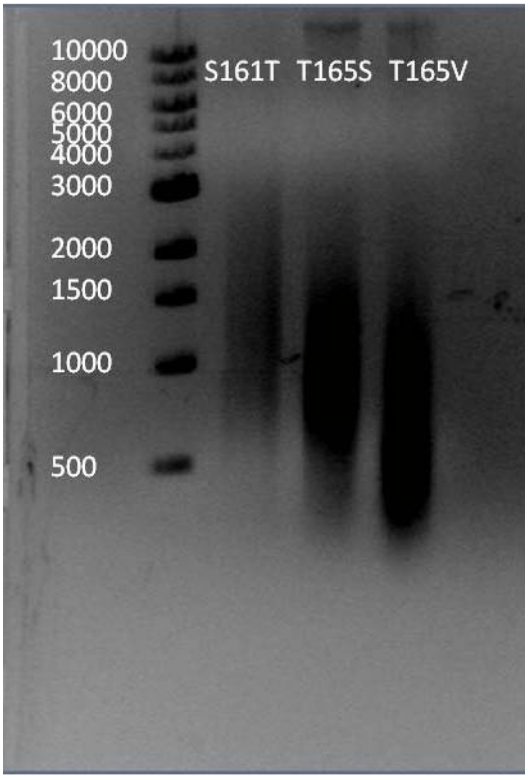

Figure 3-2. DNA Gel showing midiprep isolated DNA from QuickChange of T165S, T165V, and S161T treated with RNAse.

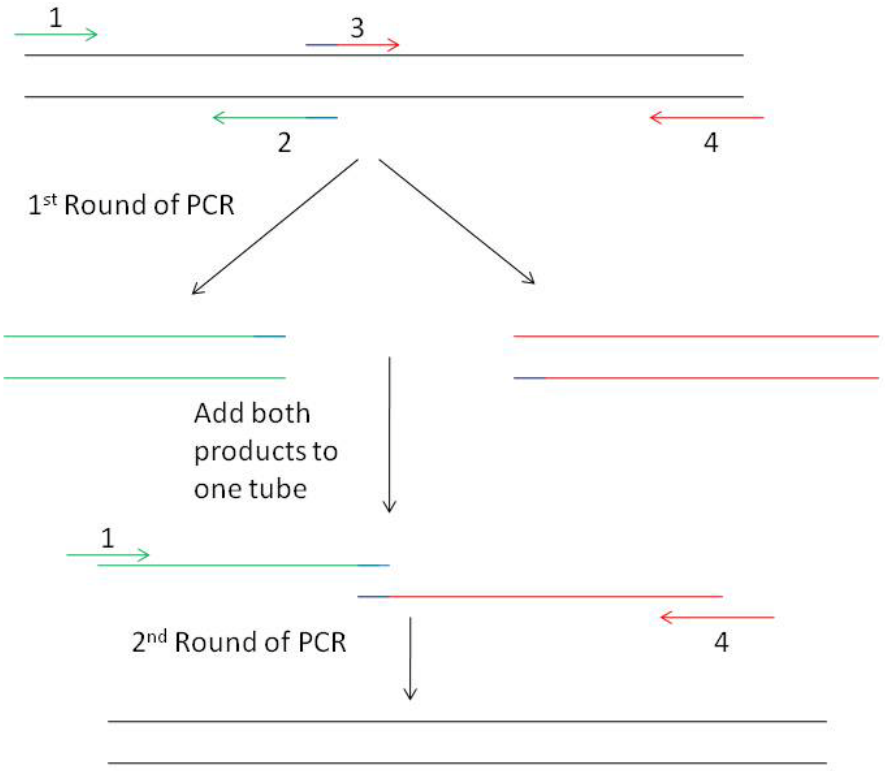

Figure 3-3. Summary of the Overlap Extension Method. The two internal primers (2 and 3) have the mutation in the blue region of the primer and also overlap about 10 base pairs in the blue region. In the first round of PCR, one tube contains the external forward primer (1 green) and the internal reverse primer (2 green) with template DNA and PCR is conducted to give the green product. In a second tube, template DNA, the forward internal primer (3 red), and the external reverse primer (4 red) are added and PCR is conducted to give the red product. In the second round, the red and green products are used as a template and the forward and reverse external primers (1 and 4) are used to extend the two pieces. This DNA is then cut and ligated into the correct vector.

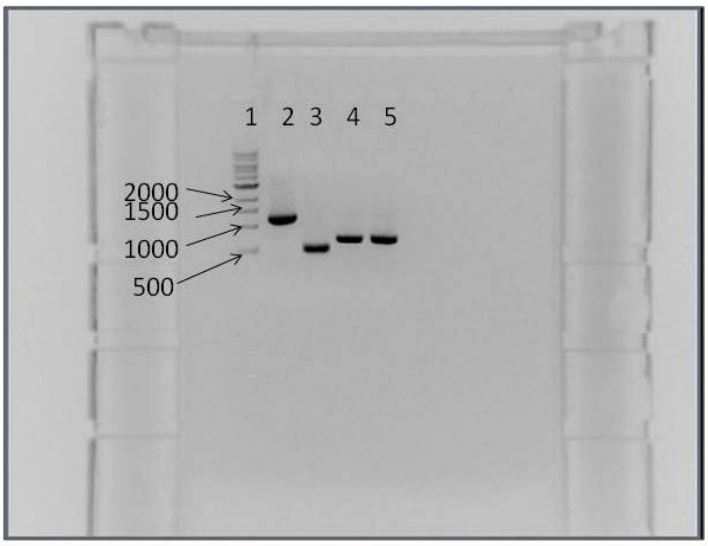

Figure 3-4. Representative gel for overlap extension mutating the His-tagged WT to T165V. The lanes are as follows: 1. 1 kbp ladder 2. PCR product obtained using forward external primer and external reverse primer using the PCR product from the first round reactions Lane 3. PCR product obtained using external forward primer and internal reverse primer Lane 4. PCR product obtained in first round of PCR using the external forward primer and internal reverse primer with the products of the first round as template Lane 5. Same as lane 4

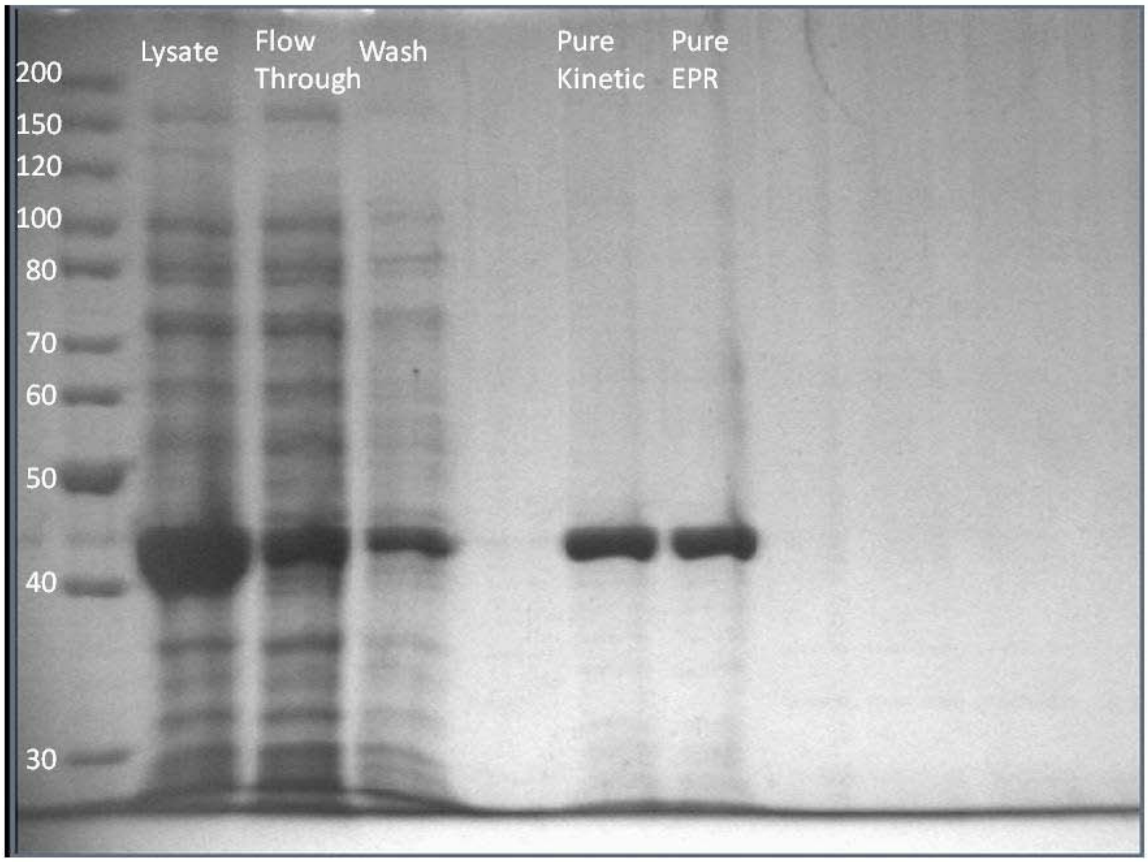

Figure 3-5. Representative 9% SDS-PAGE gel of a His-tagged WT OxDC purification.

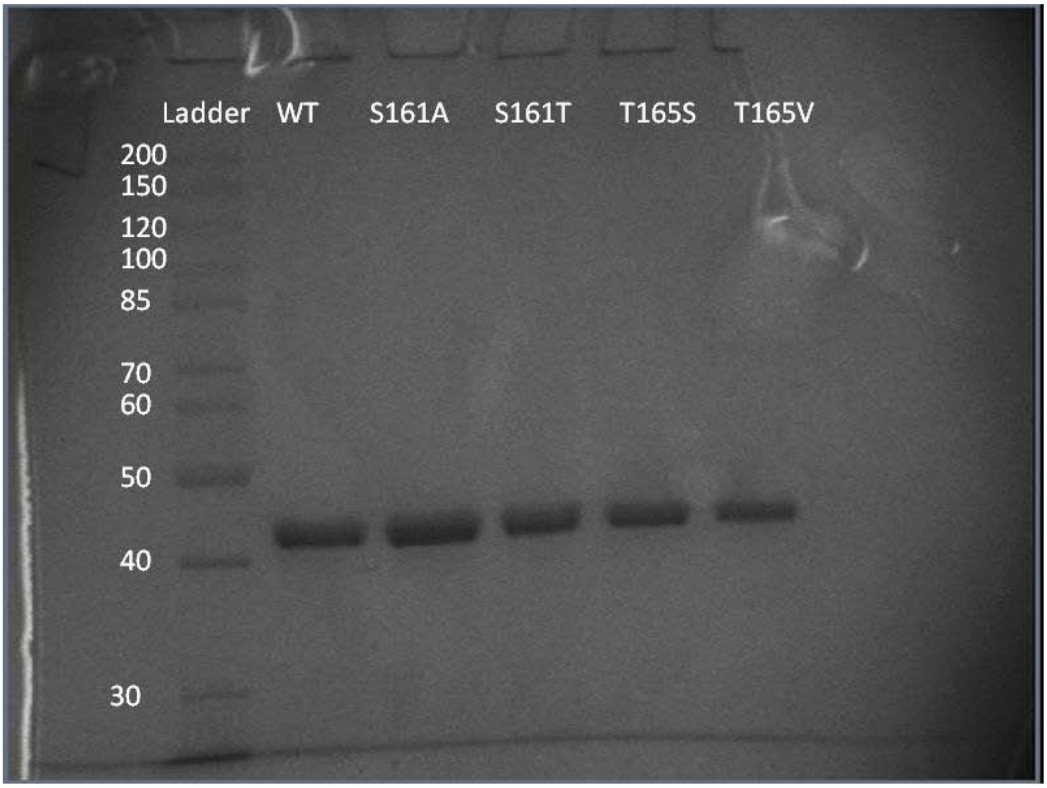

Figure 3-6. His-tagged WT and Mutant OxDC on a 9% SDS-PAGE gel all samples from the kinetic pool of protein.

Table 3-1. Summary of OxDC and mutant concentrations for EPR and kinetic assays

Enzyme	Kinetic Concentration (mg/mL)	EPR Concentration (mg/mL)	Total Amount of Protein (mg)
WT	4.7± 0.3	10.2±1	26
S161A	6.7±0.3	6.7±0.3	40
S161T	5.8±0.5	11±1	29
T165S	7.2±0.3	15±1.2	36
T165V	6.44±0.6	23±3	38

Cathode: $O_2 + 4H^+ + 4e^- \rightarrow 2H_2O$

Anode: $4\ Ag + 4\ Cl^- \rightarrow 4\ AgCl\ (s) + 4e^-$

Figure 3-7. Reactions that occur in a Clark Type Oxygen Electrode.

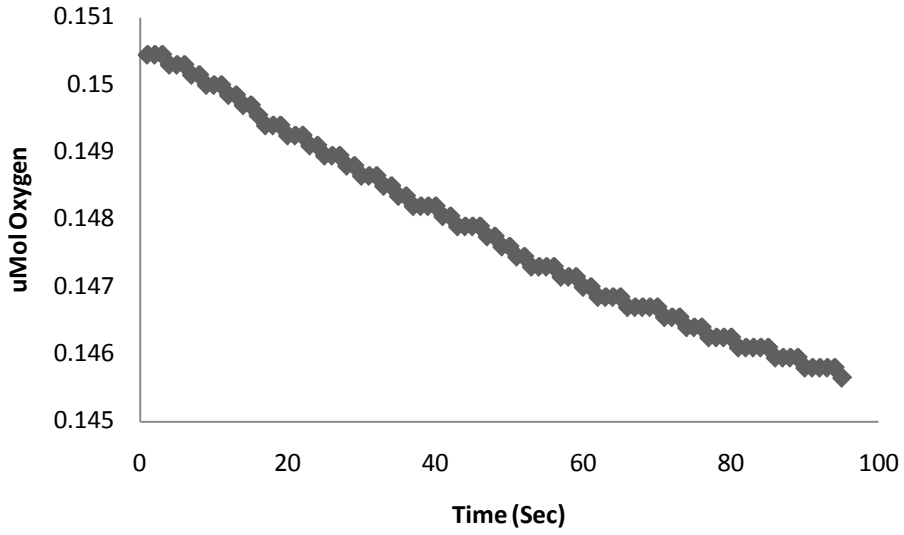

Figure 3-8. Graph showing consumption of oxygen for T165S using a Clark Type Oxygen Electrode.

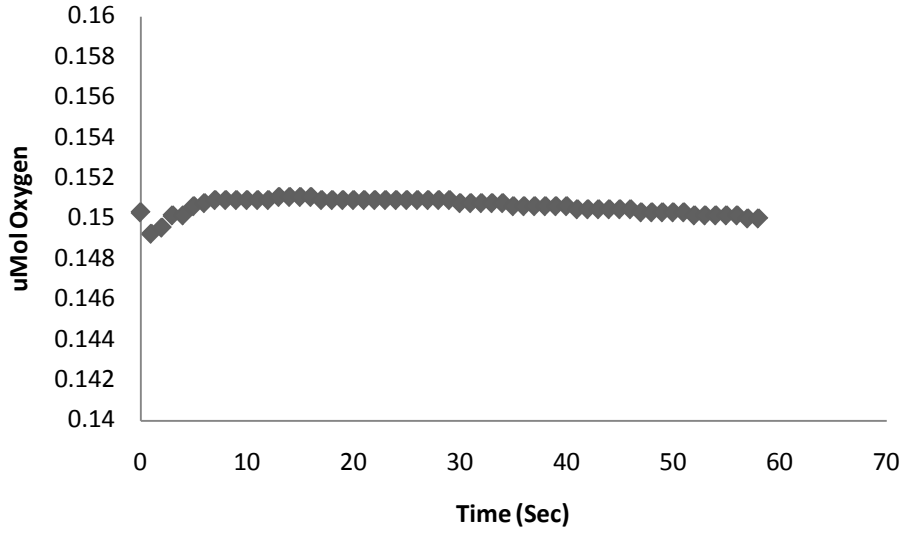

Figure 3-9. Graph showing consumption of oxygen for T165V using a Clark Type Oxygen Electrode. The drift at the time points 0-5 are due to starting the readings while the system was open during oxalate addition.

Table 3-2. Oxidase activity of T165S and T165V based on oxygen consumption using a Clark Type Electrode.

Mutant	Oxidase Activity (U/mg)
T165S	0.38±0.1
T165V	Non-detectible

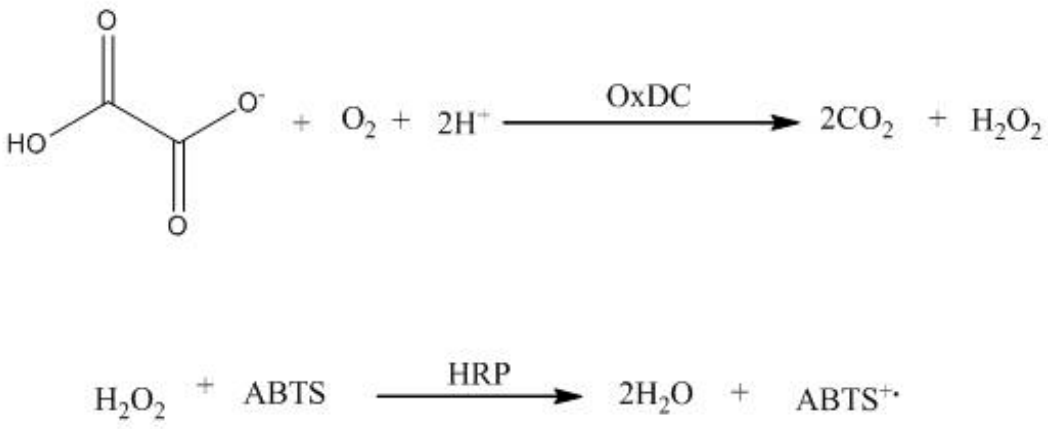

Figure 3-10. Reactions involved in the ABTS and HRP coupled oxidase assay.

Table 3-3. Oxidase activities measured by ABTS and HRP coupled assay. Reported Activities Have the Background Subtracted.

Enzyme	Specific Activity U/mg
WT Background Dye Oxidation[a]	0.22
WT	0.28 ± 0.05
S161A Background Dye Oxidation	0.47
S161A	0.27 ± 0.08
S161T Background Dye Oxidation	0.24
S161T	0.0143 ± 0.0004
T165V Background Dye Oxidation	0.0129
T165V	0.002 ± 0.001
T165S Background Dye Oxidation	0.33
T165S	0.75 ± 0.02

[a] Backgrounds are reported for the OxDC turnover mediated dye oxidation

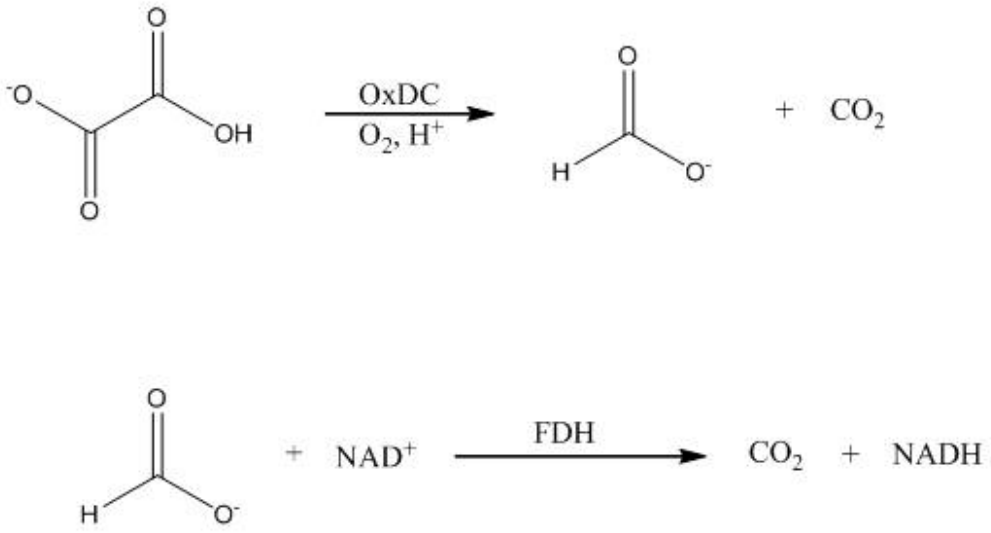

Figure 3-11. OxDC decarboxylase activity using FDH

Table 3-4. Decarboxylase and kinetic parameters for OxDC and the mutants

Enzyme	Vmax (U/mg)	Vmax (mM/min)	Km (mM)	kcat (sec-1)	kcat/Km (M-1 sec-1)	Specific Activity (U/ mg)	Metal Analysis (Mn/monomer)	U/mg/Mn
WT	40 ± 1	1.9 ± 0.07	18 ± 2	30 ±1	1600 ± 193	40 ± 0.8	1.4	21
T165V	6.1 ± 0.7	0.39 ± 0.04	30 ± 9	3.8±0.4	140 ± 46	4.6± 0.5	1.8	2.5
T165S	32 ± 3	2.00 ± 0.09	9 ± 1	20 ±0.9	2100 ± 252	23 ± 2	0.7	32
S161A	50 ± 2	3.3 ± 0.17	6 ± 1	57 ±3	6000 ± 1103	48 ± 3	1.6	30
S161T	39 ± 3	2.3 ± 0.2	21 ± 5	42 ±3.5	1900 ± 487	29 ± 1	1.5	19.3

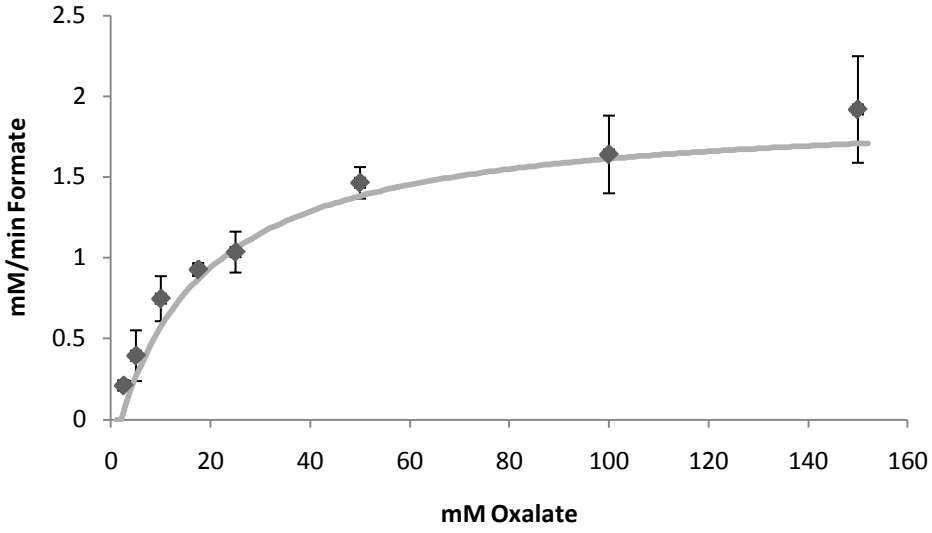

Figure 3-12. Michaelis-Menten curve for His-tagged WT OxDC

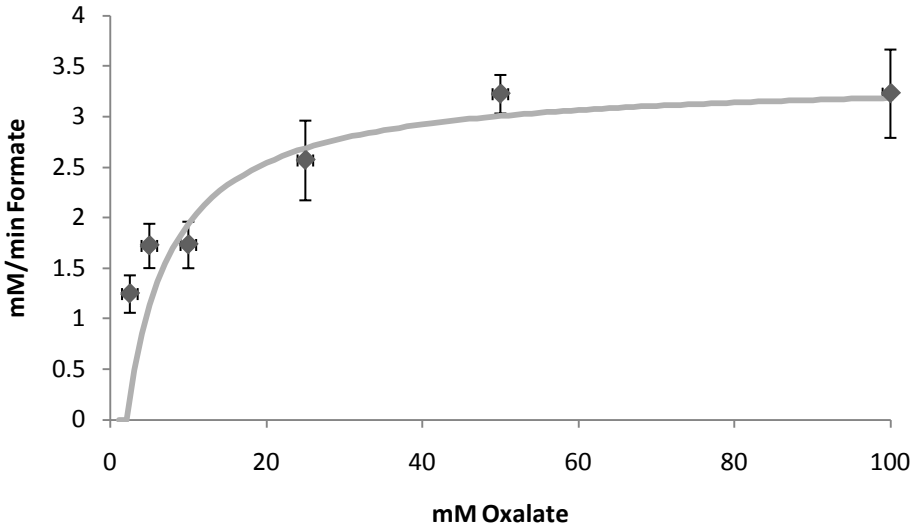

Figure 3-13. Michaelis-Menten curve for S161A

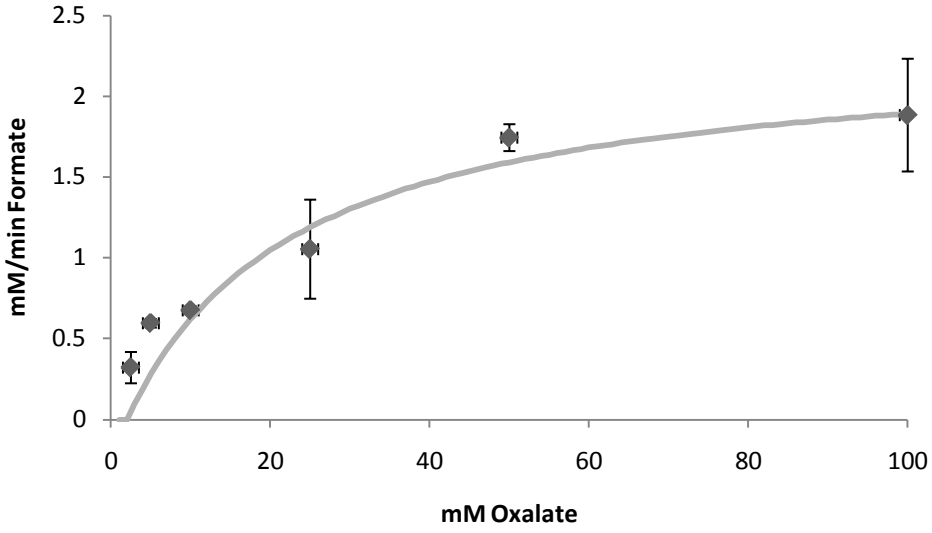

Figure 3-14. Michaelis-Menten curve for S161T

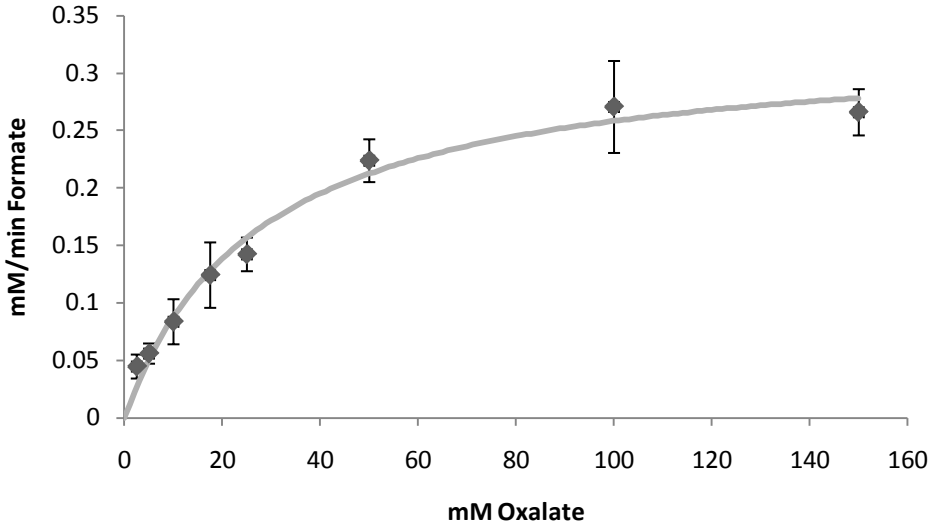

Figure 3-15. Michaelis-Menten curve for T165V

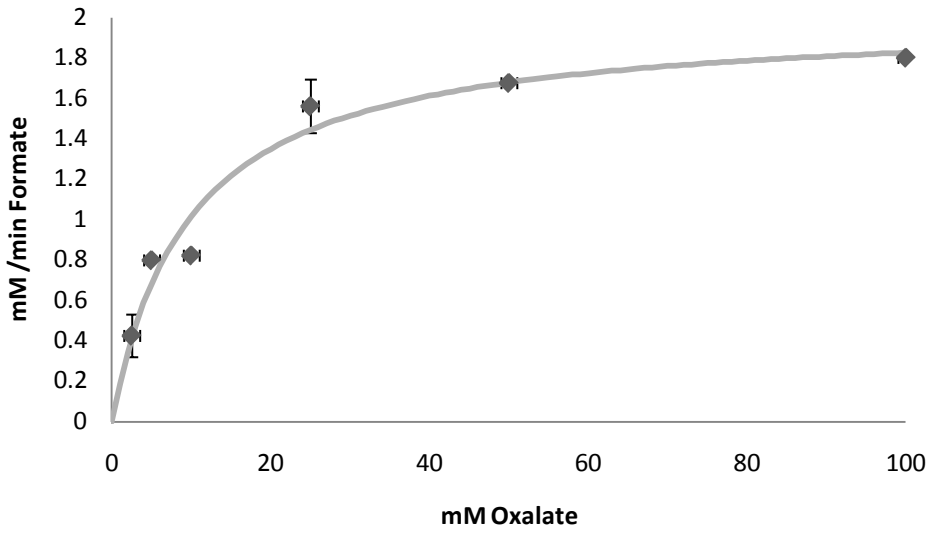

Figure 3-16. Michaelis-Menten curve for T165S

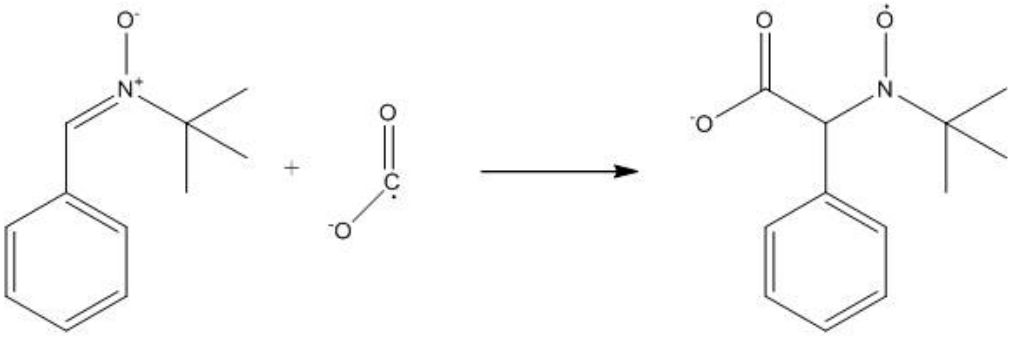

Figure 3-17. PBN spin trap reacting with a carboxyl radical

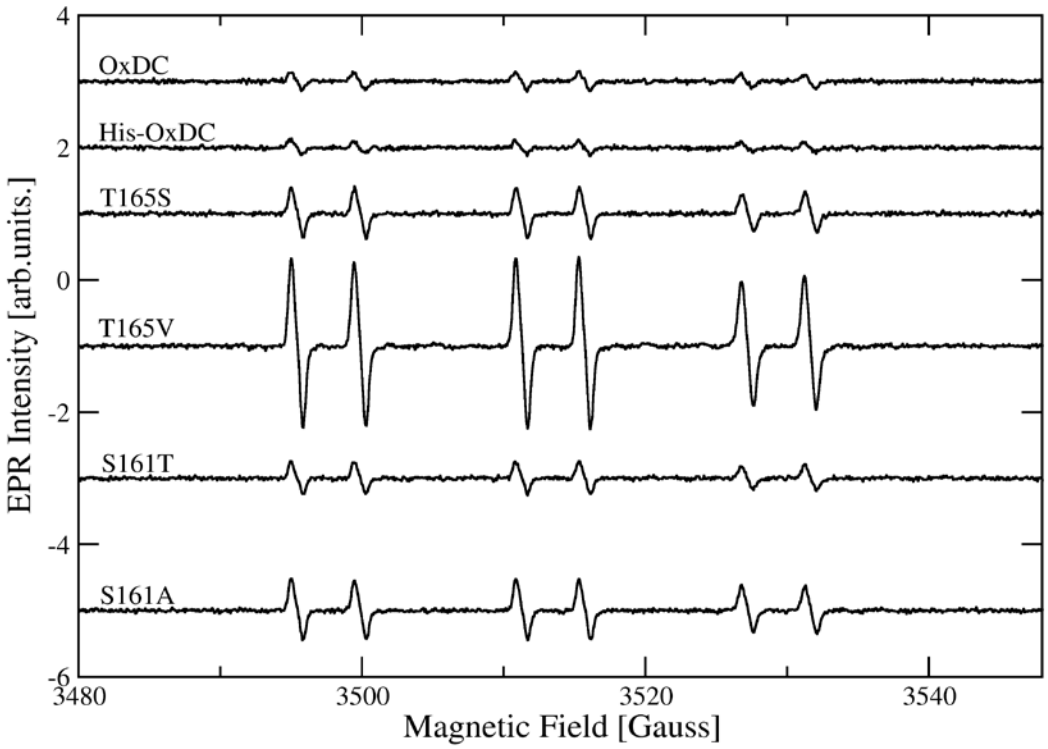

Figure 3-18. EPR of PBN spin trapping of OxDC and mutants using ^{12}C oxalate. Figure generated and provided by Witcha Imaram.

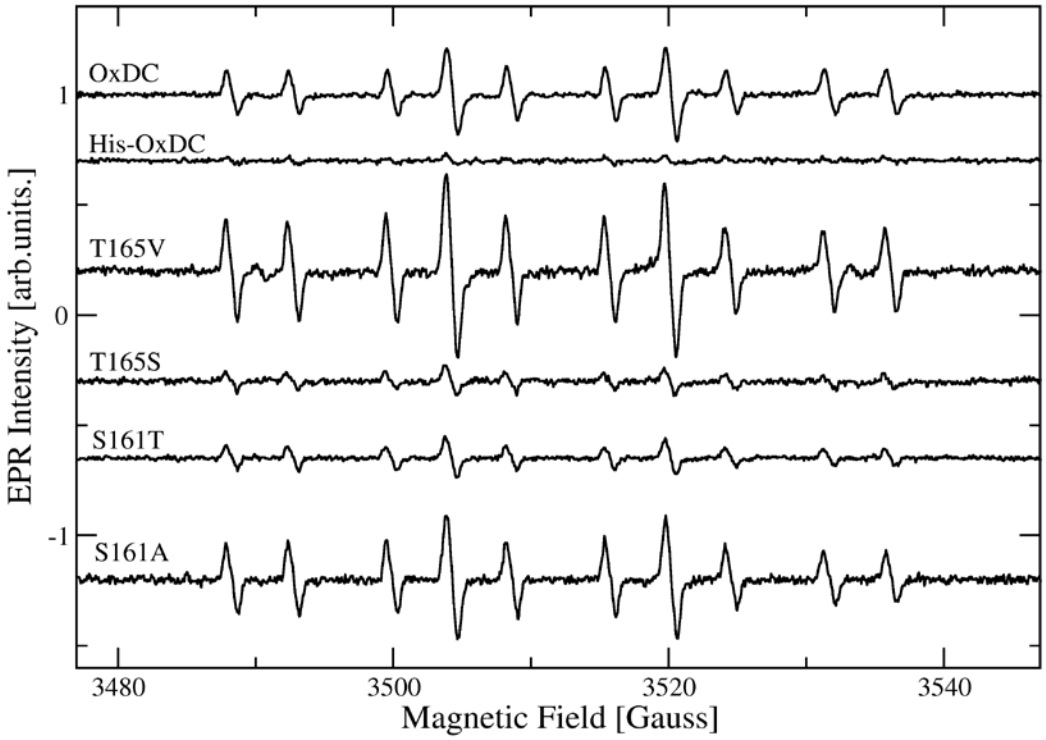

Figure 3-19. EPR of PBN spin trapping of OxDC and mutants using 13C oxalate. Figure generated and provided by Witcha Imaram

CHAPTER 4
DISCUSSION AND FUTURE WORK

Discussion

Mutagenesis Results

The QuickChange method was not successful. Only three of the mutants produced colonies. However, plasmid isolation was difficult from this method and mostly genomic DNA was isolated with no band in the gel corresponding to the expected product. This plasmid is a medium copy plasmid with only <40 copies per cell. Using LB media and the midiprep kit, not enough plasmid DNA can be isolated and most of the isolated material is sheared genomic DNA. Also, if the annealing temperature is not correct, then the PCR will fail and there is no easy way to check to see if a QuickChange PCR succeeds or fails since not enough DNA is produced to visualize on a gel. Thus, this method was abandoned in favor of the overlap extension.

The overlap extension mutagenesis was more fruitful. All four of the mutants were isolated successfully. However, there were two difficulties encountered from this method. The first was finding an annealing temperature for the first round of PCR. One mutant required a 55 ^{o}C annealing temperature and the others 60 ^{o}C. The second was screening colonies for the insert. Using LB media, no inserts were seen but using TB media about 20% of the colonies showed inserts. Once again, the LB media does not allow a high enough cell density to isolate enough plasmid DNA to visualize in a gel.

Decarboxylase Activity

The decarboxylase activity was measured for all of the mutants and the His-tagged WT enzyme. The His-tagged WT enzyme showed an activity of 40 U/mg for 1.4 Mn/monomer metal incorporation. This result is similar to what the non-tagged WT enzyme has been measured to show for similar metal incorporation. Also, the calculated K_m of 18 mM is close to the reported

value of 16 mM. This indicates that the His-tagged WT enzyme and the mutants were assayed correctly.

The S161T mutant behaved exactly like the His-tagged WT OxDC which is expected because it should participate in the H-bond network similarly to the His-tagged WT. It exhibited a specific activity of 39 U/mg for 1.5 Mn/monomer vs. the 40 U/mg for 1.4 Mn/monomer of the His-tagged WT enzyme. The K_m of 21±5 and 18±2 mM for the S161T and His-tagged WT enzyme respectively are the same within error. It appears that the extra methyl group does not affect the decarboxylase activity of the enzyme. The enzyme can probably adopt the same conformation in the closed form of the His-tagged WT enzyme.

The S161A mutant in this study also behaved similarly to the His-tagged WT OxDC. The decarboxylase activity was slightly higher than what would be predicted based on the metal incorporation. Also, the K_m of 6 mM was lower than the His-tagged WT K_m of 18 mM. This stands in stark contrast to the previous study of this mutant. Just et al. found the K_m was increased to 70 mM and the enzyme had 15% of the His-tagged WT decarboxylase activity. One of the reasons for the difference of activity in my hands could be metal incorporation. The S161A used in this study had 1.6 Mn/monomer and the previous work did not report the metal incorporation (*25*). This work confirms that the closed form of the loop does not appear to be disrupted with this mutation. If the closed form of the loop was destabilized than E162 should be rotated out of the active site lowing the decarboxylase activity. The crystal structure for S161A shows that the closed form is energetically and structurally accessible because the enzyme crystallized with the loop in the closed form. In choosing between the previous kinetic parameters and the ones in this study, I would lean towards the ones in this study. The metal

incorporation is reported, and the same solutions and techniques were used for the His-tagged WT OxDC and the His-tagged WT parameters from the literature were reproduced in this work.

The T165S had the lowest metal incorporation with 0.7 Mn/monomer. This lowered the decarboxylase activity to 23 U/mg which is what the non-tagged WT is expected to show for a similar metal loading (*14*). Also, the k_{cat}/K_m of 2100 M^{-1} sec^{-1} is very close to the His-tagged WT value of 1600 M^{-1} sec^{-1}. The K_m of 9 mM is also similar to the His-tagged WT enzyme. The lowered decarboxylase activity is due to low metal loading and not a change in the protein because the k_{cat}/K_m is similar to the His-tagged WT OxDC. The serine appears to still H-bond to R92 and helps keep it in position for catalysis to occur. Changing the threonine to a serine, does not affect the decarboxylase activity.

The T165V had only about 10% of the His-tagged WT decarboxylase activity. The T165V had 4.6 U/mg of decarboxylase activity with a metal incorporation of 1.8 Mn/monomer, the highest metal incorporation in this study. The lower activity cannot be due to lack of Mn in protein. This mutation does not disrupt the Mn binding as evidenced by the high loading. Also this mutation cannot H-bond to R92, and it is possible that with the H-bonding removed R92 is not positioned correctly for decarboxylation lowering the rate of decarboxylase activity.

Overall, the only mutation that drastically affected decarboxylase activity was the T165V. The other 3 mutants displayed kinetics that where similar to the His-tagged WT enzyme. The S161T mutant behaved exactly like the His-tagged WT enzyme and, the S161A displayed slightly increased activity. T165S when normalized for metal content behaved similarly to the His-tagged WT enzyme as well and its lower activity is due to metal loading and not the mutation disrupting the enzyme. However, the T165V was significantly different. It had much lower activity, most likely due its inability to H-bond and help stabilize and orient R92. All of

this shows that the decarboxylase activity has some dependence on the H-bonding within the loop region. The S161 does not have any crucial H-bonds the help favor decarboxylase activity over oxidase activity. Removing S161's H-bonds actually increased the rate of decarboxylase activity. But the T165 H-bonds are important. Removal of the H-bonds to R92 drops the decarboxylase activity by 90%. This points to T165 being a major residue in the loop that influences decarboxylase activity.

Oxidase Activity and Dye Oxidation Activity

The oxidase activity for the His-tagged WT OxDC and mutants was measured by examining ABTS dye oxidation from HRP. The oxidase activity had to be corrected by subtracting the background rate of dye oxidation during OxDC turnover. The oxidase activities can be broken down into three categories. The first is very low measureable oxidase activity which includes the S161T and T165V mutants. The second is His-tagged WT level oxidation and includes the His-tagged WT enzyme and S161A mutant. The last is higher than the WT oxidase activity and only includes T165S.

The T165V and S161T enzymes had very low oxidase activities. Both had activities under 0.02 U/mg. Since T165V has a low decarboxylase activity it probably produces few radicals during turnover especially if decarboxylation is difficult. Obviously, if the decarboxylation does not occur than the carboxyl radical is not produced and cannot undergo oxidation. The S161T is harder to rationalize. The decarboxylase activity is similar to His-tagged WT yet it has an oxidase activity an order of magnitude below the His-tagged WT enzyme. However, the dye oxidation activity is the same at the His-tagged WT. Since the dye oxidation is the same, the S161T is making a radical that is capable of oxidizing the dye and this radical is only present if oxalate is added.

The His-tagged WT and S161A both had similar oxidase activities of 0.28 and 0.27 U/mg respectively. Interestingly, the background dye oxidation rate of the S161A was twice the rate of the WT enzyme, 0.47 vs 0.22 U/mg. Removing the H-bonds at position 161 does not increase the oxidase activity of the enzyme. The background dye oxidation rate will increase but the oxidase activity will not. There is no obvious reason for the increased background rate. Maybe a radical is leaking out of the active site in S161A before the carboxyl radical anion is protonated. From these experiments, it is impossible to say what or how the dye gets oxidized.

The only mutant with an increased oxidase activity was T165S. This mutant had an oxidase activity of 0.75 U/mg which is three times the His-tagged WT oxidation rate. The background dye oxidation rate is 0.33 U/mg which is similar to the His-tagged WT. Once again, it is hard to rationalize why this rate is increased. The H-bond to R92 is still present, and it is possible these residues could adopt slightly different conformations along with E162 which would slow the protonation and increase oxidase activity. If this were true, it would be a very slight disruption as the normalized decarboxylase activity is very similar to the His-tagged WT enzyme.

Mutations of S161 do not increase the oxidase activity. Changing the serine to a threonine, lowers the oxidase activity and changing it to an alanine keeps the oxidase activity the same as the His-tagged WT. The H-bonding at hydroxyl position of S161 does appear to play a major role in determining the activity of the enzyme. The decarboxylase activity is similar for S161A and S161T when compared to the WT. The H-bonding network plays a small role in the oxidase activity since S161T has a decrease on oxidase activity with a similar background rate of dye oxidation during turnover. The S161A displays a similar oxidation activity as the His-tagged WT enzyme.

The T165 hydroxyl H-bonding's role in oxidation activity is easier to explain. Removing the H-bonds in the T165V mutant dropped the oxidase activity to 0.002 U/mg, a full two orders of magnitude under the His-tagged WT. This also coincided with a drop in background dye oxidation. This is possibly explained by the overall lowered activity of T165V since R92 is now hypothesized to not be positioned correctly to stimulate decarboxylation. If decarboxylation does not occur, then no carboxyl radical is produced which can undergo decarboxylase lowering the oxidase activity. Putting in a serine, which can have more rotational freedom since it lacks the methyl group, actually increases the oxidase activity three times over the His-tagged WT rate. It is possible that the T165S can adopt a slightly different conformation that allows for an increase in oxidation however, this remains to be verified.

EPR Spin Trapping

The radicals produced during turnover of the His-tagged WT and mutants were examined by EPR using PBN as a spin trap. The reaction times were varied so that each mutant consumed a similar amount of oxalate. With PBN as the spin trap, the trapped radical gave a 6 line spectrum which was the same for all enzymes. The His-tagged WT had the weakest spectrum, but all 6 lines are still visible. The T165V had the strongest spectrum.

Radical trapping with PBN was also conducted using ^{13}C oxalate. Using ^{13}C oxalate, a 10 line spectrum was recorded for all enzymes in this study. The trapped radical must originate from oxalate in order for this spectrum to be produced. If the trapped radical originated from superoxide, the ^{13}C oxalate would not change the spectrum because the radical is not derived from the oxalate would not be incorporated. Thus, the radical produced during turnover is from oxalate.

The amount of radical does not seem to be directly dependent on decarboxylase activity or oxidase activity. If it was dependent on decarboxylase activity then the S161A should have the

most radical trapped and it does not. The T165V has the most radical trapped and the His-tagged WT has the least. If it depended on the oxidase activity then T165S should have the most radical trapped but it does not. The T165V is interesting since it has the most radicals trapped. If decarboxylation is slow then low amounts of the oxalate derived radical should be trapped. This is not the case. Possibly after decarboxylation the loop opens and the PBN gains access to the intermediate carboxyl radical increasing the amount of radical trapped.

Overall Conclusions

This work has demonstrated that single point mutations at position S161 do not significantly alter the decarboxylase and oxidase activities. The S161T, not unexpectedly, behaves similarly to the His-tagged WT enzyme. This is expected since threonine is expected to have similar H-bonding interactions as serine. However, the S161A mutant was expected to behave differently because it has no hydroxyl group to participle in the H-bonds and was hypothesized to favor the open form of the loop. Yet, it has a decarboxylase activity that is slightly higher than the His-tagged WT enzyme and a lower K_m indicating that the closed form may still be favored. Neither of these mutants exhibited an increased oxidase activity. The S161T has an order of magnitude decrease in oxidase activity. The conclusion is that the H-bonding network for S161 plays a very small role determining if the enzyme has decarboxylase or oxidase activity.

The T165 does help determine if the enzyme possesses oxidase or decarboxylase activity. The T165V mutant which cannot H-bond to R92 has a tenth of the decarboxylase activity of the His-tagged WT enzyme. This is most likely due to its inability to H-bond to R92. If R92 is not in the correct location it cannot polarize oxalate prior to decarboxylation. Also, this would keep the loop open with E162 rotated away slowing down the decarboxylation reaction. With the loop open, the oxidase activity was expected to increase but this was not the case. This mutant had

drastically decreased oxidase activity. If the decarboxylation is slow than there would be less carboxyl radical formed lowering the oxidase activity.

The T165S mutant showed an increase in oxidation from 0.22 U/mg to 0.75 U/mg. Removing the methyl group somehow increased the oxidase activity of this mutant. This mutant should still be able to stabilize R92 but perhaps it adopts a slightly different conformation with the R92. This would be possible if the methyl group had steric interactions with other nearby residues. Without the methyl group, the serine would not have these steric interactions. Also, the decarboxylase activity was similar to what has been seen for the non-tagged WT enzyme with a similar metal content implying that this mutation does not significantly alter the decarboxylase activity.

The radical trapping for these mutants showed that they all generate a radical that is derived from oxalate. When ^{13}C oxalate is used, the spectrum goes from 6 lines to 10 lines. If the radical was from superoxide the ^{13}C oxalate spectrum should be the same as the ^{12}C oxalate.

Overall, the mutants that were proposed to favor the open form of the loop, S161A and T165V, did not increase the oxidase activity. The hypothesis for this work was that favoring the open form of the loop should increase the oxidase activity since E162 is rotated away which would make protonation of the carboxyl radical anion difficult leading to an increase in oxidase activity. This was not seen. The T165V is fairly easy to explain since it cannot H-bond to R92, it is expected that R92 might not be positioned correctly to facilitate the decarboxylation of oxalate. If the decarboxylation is slow than it is expected that oxidase activity would be slowed as well. It is not obvious why S161A would have similar reactivity to the His-tagged WT. The most likely explanation is that S161 despite having an extensive H-bonding network in the closed form is not important in determining the reactivity of the enzyme, and the S161A loop is

stable in the closed from so E162 can protonate the carboxyl radical anion. Overall, single point mutations that affect the H-bond network are not enough to change the specificity of the enzyme. There must be other factors that contribute to the specificity for OxDC to be a decarboxylase.

Future Work

This work has shown that residue T165 is important in determining OxDC activity. Mutations at this position can significantly drop decarboxylase activity or slightly increase the oxidase activity. The mechanism by which this occurs was not determined. Much of the future work should be focused on understanding the T165 mutant.

The first project that should be conducted involves computational studies on the loop. It would be important to know what an energy minimized structure of the closed loop would look like and how the mutations at T165 would affect the orientation of residues in the closed loop. This would show if the R92 is moved in the T165S or if the hydroxyl group is rotated and has a slightly different H-bond arrangement. Once this is done and there is an energy minimized closed loop structure, calculations should be done on the energies of the decarboxylase and oxidase reactions. These calculations could be compared to the His-tagged WT enzyme calculations and should shed some light on the different reactivity of this mutant. Calculations on S161A would be fruitful as well. Since there is disagreement between this work and the literature, it would be important to know the energies of the active site in the closed form and compare them to the WT. If it is similar to the His-tagged WT then S161A would be expected to have similar activity to the His-tagged WT enzyme.

Another interesting computational study would involve the T165V mutant. For this mutant, calculations should focus on the loop energy. The energy of the His-tagged WT closed form could be compared to the closed from of T165V to find out how much stabilization energy the H-bonds from T165 provides. This should also allow for a model structure to be created that

would show where R92 would be positioned in the closed from of the T165V loop. This would elucidate exactly where R92 has to be placed for decarboxylation to occur and where it is placed in the T165V mutant.

A second project would involve construction and analysis of a few more mutants. Previous work has shown that E162Q has an increased oxidase activity. It would be interesting to see what happens when this mutation is paired with a T165S mutation. This mutant would be expected to exhibit higher oxidase activity because both residues have been shown on their own to increase the oxidase activity.

A third project would be to get crystal structures of the three new mutants. The most interesting crystal structure would be the closed form of T165S. This could provide insight into the structure of the closed form of the mutated loop and could be compared to the computational results. Hopefully, the changes in the active site would provide an explanation of the higher oxidase activity that is seen with this mutant. A closed from of T165V could show if the R92 is moved into a different position; however, this mutant would be hard/impossible to crystallize in the closed form if this mutant strongly favors the open form. In addition, the closed form appears to be destabilized since the decarboxylase activity for this mutant is much lower than the His-tagged WT. A crystal structure of S161T would mostly be interesting to see if it favors crystallization in the open or closed form and to see if it binds formate in the closed loop position like S161A.

LIST OF REFERENCES

1. Dutton, M. V., and Evans, C. S. (1996) Oxalate production by fungi: Its role in pathogenicity and ecology in the soil environment. *Canadian Journal of Microbiology 42*, 881–895.

2. P. Magro, P. M. P. L. (1988) Enzymatic oxalate decarboxylation in isolates of Sclerotinia sclerotiorum. *FEMS Microbiology Letters 49*, 49–52.

3. Lillehoj, E. B., and Smith, F. G. (1965) An Oxalic Acid Decarboxylase of Myrothecium Verrucaria. *Archives of Biochemistry and Biophysics 109*, 216–218.

4. Emiliani, E., and Riera, B. (1968) Enzymatic Oxalate Decarboxylation in Aspergillus Niger.2. Hydrogen Peroxide Formation and Other Characteristics of Oxalate Decarboxylase. *Biochimica Et Biophysica Acta 167*, 414–419.

5. Emiliani, E., and Bekes, P. (1964) Enzymatic Oxalate Decarboxylation in Aspergillus Niger. *Archives of Biochemistry and Biophysics 105*, 488.

6. Tanner, A., and Bornemann, S. (2000) Bacillus subtilis YvrK is an acid–induced oxalate decarboxylase. *Journal of Bacteriology 182*, 5271–5273.

7. Tanner, A., Bowater, L., Fairhurst, S. A., and Bornemann, S. (2001) Oxalate decarboxylase requires manganese and dioxygen for activity - Overexpression and characterization of Bacillus subtilis YvrK and YoaN. *Journal of Biological Chemistry 276*, 43627–43634.

8. Tanner, A., and Bornemann, S. (2001) The metal ion cofactor of Bacillus subtilis oxalate decarboxylase is Mn(II). *Journal of Inorganic Biochemistry 86*, 450–450.

9. Dunwell, J. M. (1998) Cupins: A new superfamily of functionally diverse proteins that include germins and plant storage proteins. *Biotechnology & Genetic Engineering Reviews, Vol. 15 15*, 1–32.

10. Dunwell, J. M., Purvis, A., and Khuri, S. (2004) Cupins: the most functionally diverse protein superfamily? *Phytochemistry 65*, 7.

11. Dunwell, J. M., Culham, A., Carter, C. E., Sosa-Aguirre, C. R., and Goodenough, P. W. (2001) Evolution of functional diversity in the cupin superfamily. *Trends in Biochemical Sciences 26*, 740.

12. Burrell, M. R. (2006) in *Biological Chemistry* pp 176, University of East Anglia, Norwich.

13. Just, V. J., Stevenson, C. E. M., Bowater, L., Tanner, A., Lawson, D. M., and Bornemann, S. (2004) A closed conformation of Bacillus subtilis oxalate decarboxylase OxdC provides evidence for the true identity of the active site. *Journal of Biological Chemistry 279*, 19867–19874.

14. Moomaw, E. W. (2007) in *Chemistry* pp 117, University of Florida, Gainesville.

15. Burrell, M. R., Just, V. J., Bowater, L., Fairhurst, S. A., Requena, L., Lawson, D. M., and Bornemann, S. (2007) Oxalate decarboxylase and oxalate oxidase activities can be interchanged with a specificity switch of up to 282 000 by mutating an active site lid. *Biochemistry 46*, 12327–12336.

16. Angerhofer, A., Moomaw, E. W., Garcia-Rubio, I., Ozarowski, A., Krzystek, J., Weber, R. T., and Richards, N. G. J. (2007) Multifrequency EPR studies on the Mn(II) centers of oxalate decarboxylase. *Journal of Physical Chemistry B 111*, 5043–5046.

17. Moomaw, E. W., Angerhofer, A., Moussatche, P., Ozarowski, A., Garcia-Rubio, I., and Richards, N. G. J. (2009) pp 39.

18. Svedruzic, D., Liu, Y., Reinhardt, L. A., Wroclawska, E., Cleland, W. W., and Richards, N. G. J. (2007) Investigating the roles of putative active site residues in the oxalate decarboxylase from Bacillus subtilis. *Archives of Biochemistry and Biophysics 464*, 36–47.

19. Anand, R., Dorrestein, P. C., Kinsland, C., Begley, T. P., and Ealick, S. E. (2002) Structure of oxalate decarboxylase from Bacillus subtilis at 1.75 angstrom resolution. *Biochemistry 41*, 7659–7669.

20. Requena, L., and Bornemann, S. (1999) Barley (Hordeum vulgare) oxalate oxidase is a manganese-containing enzyme. *Biochemical Journal 343*, 185–190.

21. Kotsira, V. P., and Clonis, Y. D. (1997) Oxalate oxidase from barley roots: Purification to homogeneity and study of some molecular, catalytic, and binding properties. *Archives of Biochemistry and Biophysics 340*, 239–249.

22. Woo, E. J., Dunwell, J. M., Goodenough, P. W., and Pickersgill, R. W. (1998) Barley oxalate oxidase is a hexameric protein related to seed storage proteins: evidence from X-ray crystallography. *Febs Letters 437*, 87–90.

23. Escutia, M. R., Bowater, L., Edwards, A., Bottrill, A. R., Burrell, M. R., Polanco, R., Vicuna, R., and Bornemann, S. (2005) Cloning and Sequencing of two Ceriporiopsis subvermispora bicupin oxalate oxidase allelic isoforms: Implications for the reaction specificity of oxalate oxidases and decarboxylases. *Applied and Environmental Microbiology 71*, 3608–3616.

24. Aguilar, C., Urzua, U., Koenig, C., and Vicuna, R. (1999) Oxalate oxidase from Ceriporiopsis subvermispora: Biochemical and cytochemical studies. *Archives of Biochemistry and Biophysics 366*, 275–282.

25. Just, V. J., Burrell, M. R., Bowater, L., McRobbie, I., Stevenson, C. E. M., Lawson, D. M., and Bornemann, S. (2007) The identity of the active site of oxalate decarboxylase and the importance of the stability of active-site lid conformations. *Biochemical Journal 407*, 397–406.

26. DeLano, W. L. (2002), Delano Scientific.

27. Thompson, J. D., Higgins, D. G., and Gibson, T. J. (1994) Clustal-W - Improving the Sensitivity of Progressive Multiple Sequence Alignment through Sequence Weighting, Position-Specific Gap Penalties and Weight Matrix Choice. *Nucleic Acids Research 22*, 4673–4680.

28. (2004) *QuickChange site direted mutagenesis kit instruction manual*, Stratagene., La Jolla, CA

29. Ho, S. N., Hunt, H. D., Horton, R. M., Pullen, J. K., and Pease, L. R. (1989) Site-Directed Mutagenesis by Overlap Extension Using the Polymerase Chain-Reaction. *Gene 77*, 51–59.

30. Maniatis, T., Sambrook, J., and Fritsch, E. F. (1989) *Molecular cloning a laboratory manual*, Vol. 1, 2nd ed., Cold Springs Harbor Laboratory Press, Cold Springs Harbor, NY.

31. Bradford, M. M. (1976) A Rapid and Sensitive Method for Quantitation of Microgram Quantities of Protein Utilizing the Principle of Protein-Dye Binding. *Analytical Biochemistry 72*, 248–254.

32. Clark, L. C. (1956) Monitor and Control of Blood and Tissue Oxygen Tensions. *Transactions American Society for Artificial Internal Organs 2*, 41–43.

33. Chappell, J. B. (1964) Oxidation of Citrate Isocitrate + Cis-Aconitate by Isolated Mitochondria. *Biochemical Journal 90*, 225–228.

34. Lavallie, E. R., Diblasio, E. A., Kovacic, S., Grant, K. L., Schendel, P. F., and Mccoy, J. M. (1993) A Thioredoxin Gene Fusion Expression System That Circumvents Inclusion Body Formation in the Escherichia-Coli Cytoplasm. *Bio-Technology 11*, 187–193.

35. Skoog, D. A., Holler, J. F., and Nieman, T. A. (1998) *Principles of instrumental analysis fifth edition*, 5th ed., Brooks/Cole Thompson Learning.

36. (1999) *Instech Dissolved Oxygen Measuring System 203 Operation Manual*, Plymouth Meeting, PA.

37. Svedruzic, D., Jonsson, S., Toyota, C. G., Reinhardt, L. A., Ricagno, S., Linqvist, Y., and Richards, N. G. J. (2005) The enzymes of oxalate metabolism: unexpected structures and mechanisms. *Archives of Biochemistry and Biophysics 433*, 176–192.

BIOGRAPHICAL SKETCH

Benjamin Thomas Saylor was born in Knoxville, Tennessee in November of 1982. He graduated Summa Cum Laude from East Tennessee State University with a Bachelor of Science Degree in American Chemical Society Chemistry in 2005. After graduation, he pursued his master's degree at the University of Florida under the tutelage or Nigel Richards. Ben also has a twin brother.